



## Review

# Effect of nanoparticle shape on the performance of thermal systems utilizing nanofluids: A critical review



Iman Zahmatkesh<sup>a</sup>, Mikhail Sheremet<sup>b</sup>, Liu Yang<sup>c</sup>, Saeed Zeinali Heris<sup>d</sup>, Mohsen Sharifpur<sup>e</sup>, Josua P. Meyer<sup>e</sup>, Mohammad Ghalambaz<sup>f,g</sup>, Somchai Wongwises<sup>h,i</sup>, Dengwei Jing<sup>j,\*</sup>, Omid Mahian<sup>k,l,\*\*</sup>

<sup>a</sup> Department of Mechanical Engineering, Mashhad Branch, Islamic Azad University, Mashhad, Iran

<sup>b</sup> Laboratory on Convective Heat and Mass Transfer, Tomsk State University, Tomsk 634050, Russia

<sup>c</sup> Key Laboratory of Energy Thermal Conversion and Control of Ministry of Education, School of Energy and Environment, Southeast University, Nanjing, 210096, China

<sup>d</sup> Faculty of Chemical and Petroleum Engineering, University of Tabriz, Tabriz, Iran

<sup>e</sup> Department of Mechanical and Aeronautical Engineering, University of Pretoria, Pretoria 0002, South Africa

<sup>f</sup> Metamaterials for Mechanical, Biomechanical and Multiphysical Applications Research Group, Ton Duc Thang University, Ho Chi Minh City, Vietnam

<sup>g</sup> Faculty of Applied Sciences, Ton Duc Thang University, Ho Chi Minh City, Vietnam

<sup>h</sup> Department of Mechanical Engineering, Faculty of Engineering, King Mongkut's University of Technology Thonburi (KMUTT), Bangkok 10140, Thailand

<sup>i</sup> National Science and Technology Development Agency (NSTDA), Pathum Thani 12120, Thailand

<sup>j</sup> International Research Center for Renewable Energy, Xi'an Jiaotong University, Xi'an, Shanxi 710049, China

<sup>k</sup> School of Chemical Engineering and Technology, Xi'an Jiaotong University, Xi'an, Shanxi 710049, China

<sup>l</sup> Renewable Energy and Micro/Nano Sciences Lab., Department of Mechanical Engineering, Ferdowsi University of Mashhad, Mashhad, Iran

## ARTICLE INFO

## Article history:

Received 1 June 2020

Received in revised form 21 September 2020

Accepted 23 September 2020

Available online 13 October 2020

## Keywords:

Nanofluid

Nanoparticle shape

Convection heat transfer

Pumping power

Hydrothermal performance

## ABSTRACT

Due to their superior thermophysical properties, there is a growing body of work on nanofluids in the field of thermal systems. However, there is no specific review of the role of the nanoparticle shape, which has been found crucial to their performance adjustment. A comprehensive literature review of the effect of nanoparticle shape on the hydrothermal performance of thermal systems utilizing nanofluids was compiled. The review covered the forced, mixed, and natural convection regimes and included heat exchangers, boundary layer flows, channel flows, peristaltic flows, impinging jets, cavity flows, and flows of hybrid nanofluids. It indicated that the control of nanoparticle shape is a promising technique for the optimization of heat exchange and the required pumping power. However, no uniform conclusion was reached for the role of nanoparticle shape on the hydrothermal performance of thermal systems. In most of the previous studies in the natural and forced convection regimes, the platelet-like nanoparticle acquired the highest heat transfer rate. However, most of the works in the mixed convection regime reported the best heat transfer performance for the blade-like nanoparticle. More research studies are required in future to determine the role of nanoparticle shape for thermal management of energy systems.

© 2020 Published by Elsevier B.V.

## Contents

1. Introduction . . . . .	2
2. Nanoparticle shapes . . . . .	3
3. Models for the incorporation of the nanoparticle shape effect . . . . .	4
3.1. Thermal conductivity . . . . .	5
3.2. Dynamic viscosity . . . . .	5
3.3. Discussion . . . . .	6
4. Nanoparticle shape effect in the forced convection regime . . . . .	7
4.1. Boundary layer flow . . . . .	7
4.2. Channel flow . . . . .	7

\* Corresponding author.

\*\* Correspondence to: O. Mahian, School of Chemical Engineering and Technology, Xi'an Jiaotong University, Xi'an, Shanxi 710049, China.

E-mail addresses: [Zahmatkesh5310@mshdiau.ac.ir](mailto:Zahmatkesh5310@mshdiau.ac.ir) (I. Zahmatkesh), [mohammad.ghalambaz@tdtu.edu.vn](mailto:mohammad.ghalambaz@tdtu.edu.vn) (M. Ghalambaz), [dwjing@xjtu.edu.cn](mailto:dwjing@xjtu.edu.cn) (D. Jing), [omid.mahian@xjtu.edu.cn](mailto:omid.mahian@xjtu.edu.cn) (O. Mahian).

4.3.	Impinging jets . . . . .	8
4.4.	Cavity flow . . . . .	8
4.5.	Flow in heat exchangers . . . . .	8
5.	Nanoparticle shape effect in the mixed convection regime . . . . .	9
5.1.	Peristaltic flow . . . . .	9
5.2.	Boundary layer flow . . . . .	11
5.3.	Cavity flow . . . . .	12
5.4.	Other flow problems. . . . .	12
6.	Nanoparticle shape effect in the natural convection regime. . . . .	12
6.1.	Boundary layer flow . . . . .	12
6.2.	Cavity flow . . . . .	12
6.3.	Other flow problems. . . . .	13
7.	Nanoparticle shape effect in hybrid nanofluids . . . . .	13
7.1.	Forced convection regime . . . . .	13
7.2.	Mixed convection regime . . . . .	13
7.3.	Natural convection regime . . . . .	13
8.	Discussion. . . . .	14
9.	Concluding remarks and future works . . . . .	14
	Declaration of competing interest. . . . .	14
	Acknowledgment . . . . .	14
	References . . . . .	15

## Nomenclature

Ag	silver
$A_1, A_2$	constant coefficients
$Al_2O_3$	aluminum oxide (alumina)
$C$	specific heat
$CaCl_2$	calcium chloride
Cu	copper
$C_k$	thermal conductivity enhancement coefficient
$C_k^{shape}$	coefficient standing for the role of nanoparticle shape on thermal conductivity
$C_k^{surface}$	coefficient standing for the role of surface resistance on thermal conductivity
$d_p$	diameter of nanoparticles
$f$	empirical function
$H_2O$	water
$k$	thermal conductivity
$k_B$	Boltzmann constant
KAC	potassium acetate
$\dot{m}$	mass flow rate
$MoS_2$	molybdenum disulphide
$n$	shape factor
$Ra$	Rayleigh number
$Re$	Reynolds number
SiC	silicon carbide
$SiO_2$	silicon dioxide
$T$	temperature
$TiO_2$	titanium oxide
ZnO	zinc oxide

## Greek symbols

$\gamma-AlOOH$	boehmite alumina
$\mu$	dynamic viscosity
$\rho$	density
$\sigma$	empirical function
$\phi$	volume fraction of nanoparticles
$\psi$	sphericity

## Subscripts

Brownian	related to Brownian motion
eff	effective nanofluid property

f	base fluid
p	nanoparticle
st	static

## Abbreviations

EG	ethylene glycol
GNPs	graphene nanoplatelets
GO	graphene oxide
H-C	Hamilton–Crosser model
HFE	human engineered fluid
K-K	Koo–Kleinstreuer model
MHD	magnetohydrodynamics
MWCNTs	multi-walled carbon nanotubes
NEIL	nanoparticle enhanced ionic liquid
PEC	performance evaluation criteria
PG	propylene glycol
SWCNTs	single-walled carbon nanotubes

## 1. Introduction

Nanofluids have been discovered as novel working fluids, which are produced through dispersion of nanoparticles into a base fluid. Owing to high thermal conductivity of the added nanoparticles compared to common liquids (see Fig. 1), nanofluids are advantageous in improving thermophysical properties and elevating the convective heat transfer rate in comparison with conventional heat transfer fluids. Thus, it is not surprising to see a growing body of work on nanofluids in the field of thermal systems.

Latest developments in the modeling and simulation of nanofluid flows were reviewed by Mahian et al. [1,2] who state that a deep knowledge about hydrothermal performance of nanofluids and the parameters affecting it, is of importance in heat transfer applications.

The consequence of type, size, and loading of the nanoparticles, base fluid material, temperature, presence of surfactant, and pH level on the thermophysical properties of nanofluids was discussed in the works of Paul et al. [3], Zahmatkesh [4], Esfe et al. [5], Ghaffarkhah et al. [6], Dadwal and Joy [7], and Sharifi et al. [8,9].

Furthermore, the consequence of the abovementioned parameters on the performance of various thermal systems utilizing nanofluids

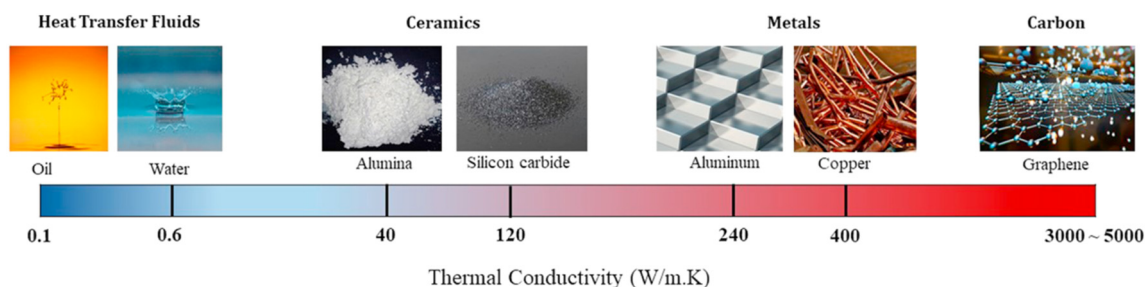


**Fig. 1.** Comparison of the thermal conductivity of conventional solids and liquids [1]. (Reprinted with permission from Elsevier)

were noted by Paul et al. [10], Bakthavatchalam et al. [11], Ghalandari et al. [12], Abbas et al. [13], Ghalambaz et al. [14], and Zahmatkesh et al. [15–20].

Although the above effects are important, experimental evidence demonstrates that the shape of the nanoparticle can also alter thermal conductivity and dynamic viscosity of the resulting nanofluid.

Xie et al. [21] were the first to report thermal conductivity alternation due to the shape of the silicon carbide (SiC) nanoparticles suspended in water or ethylene glycol. Addition of the nanoparticles having cylindrical and spherical shapes with the loading of 4 vol% revealed a thermal conductivity enhancement of 22.9% and 18.5%, respectively. The higher conductivity of the cylindrical nanoparticles was most probably due to their higher aspect ratio (nanoparticle surface area divided by its volume) than that of the spherical ones.

The rod-shaped (cylindrical) and spherical nanoparticle shapes were also discussed in the study of Murshed et al. [22] for TiO<sub>2</sub>–water nanofluid. Similar to Xie et al. [21], they reported the dependency of thermal conductivity enhancement of nanofluids to the nanoparticle shape in such a way that the cylindrical nanoparticles led to a higher thermal conductivity than the spherical ones.

Timofeeva et al. [23] experimentally examined the consequence of nanoparticle shape on thermal conductivity and dynamic viscosity of alumina nanofluids. Comparison of the results of the blade, platelet, cylindrical, brick, and spherical-shaped boehmite alumina ( $\gamma$ -AlOOH) nanoparticles dispersed in a fluid consisting of equal volumes of ethylene glycol and water revealed that the highest thermal conductivity occurred for the cylindrical nanoparticles while the lowest dynamic viscosity (i.e., lowest pumping power) occurred for the spherical-shaped nanoparticles. Based on their evidences, they proposed two correlations for thermal conductivity and dynamic viscosity of nanofluids containing different shapes of boehmite alumina nanoparticles dispersed in the ethylene glycol–water mixture.

Singh et al. [24] studied the consequences of SiC nanoparticles with platelet, cylindrical, or spherical shapes on thermal conductivity enhancement. Maximum elevation was reported for the platelet nanoparticles.

Jeong et al. [25] discussed the nanoparticle shape effect on the dynamic viscosity and thermal conductivity of zinc oxide (ZnO) nanofluids. They found that the dynamic viscosity and thermal conductivity of the nanofluid having rectangular-shaped nanoparticles were higher than those with spherical nanoparticles.

Yu et al. [26] reported the outcomes of measurement of thermal conductivity and dynamic viscosity of liquid paraffin-based suspensions in the presence of short MWCNTs, long MWCNTs, carbon nanofibers, or GNPs. The highest thermal conductivity was reported for GNPs. This was attributed to their low thermal surface resistance due to their two-dimensional planar morphology with large contact area. Utilization of the GNPs also led to the lowest value of dynamic viscosity.

Fang et al. [27] focused on the improvement of thermal conductivity of ethylene glycol through suspending silver nanoparticles with wire, flake, or spherical shapes. The nanowires with high aspect ratio caused up to about 15.6% elevation in thermal conductivity whereas the other

two shapes of nanoparticles improved the thermal conductivity up to about 5%. Moreover, they stated that the presence of the nanowires substantially raised the fluid viscosity.

Kim et al. [28] studied the suspension stability and thermophysical properties of boehmite alumina–water nanofluid having various nanoparticle shapes. At the nanoparticle volume fraction of 7%, up to about 16, 28, and 23% thermal conductivity elevations were recorded for changing the spherical nanoparticles to the blade, brick, and platelet nanoparticle shapes, respectively. They reported that thermal conductivity was associated with the stability of the nanofluid that was dependent to the shape of the dispersed nanoparticles.

The consequence of nanoparticle shape on thermal conductivity and dynamic viscosity of TiO<sub>2</sub>–water nanofluid was analyzed by Maheshwary et al. [29]. They compared the results of cube (brick), rod (cylindrical), and spherical-shaped nanoparticles and reported the highest thermal conductivity for the cylindrical nanoparticles and the lowest dynamic viscosity for the spherical ones. More recently, they extended their work to CuO, MgO, TiO<sub>2</sub>, ZrO<sub>2</sub>, and Al<sub>2</sub>O<sub>3</sub> nanoparticles [30].

Zhang et al. [31] reported the outcomes of measurement of thermal conductivity of silver–water nanofluids having nanowires or spherical nanoparticles. At the nanoparticle volume fraction of 0.46%, the thermal conductivities of nanofluid containing nanowires and nanofluid containing spherical nanoparticles were 0.2843 W/m.K and 0.2619 W/m.K, respectively.

More recently, the alternation of thermophysical properties of molten salt due to the addition of the cylindrical and spherical-shaped alumina nanoparticles was discussed by Nithiyantham et al. [32]. The experimental measurements demonstrated 12% and 16% elevations in thermal conductivity in conjunction with 37% and 25% rises in the fluid viscosity due to the addition of 1 wt% of the cylindrical and spherical-shaped alumina nanoparticles, respectively.

The shape of the nanoparticles has exhibited prominent consequences on the hydrothermal performance of thermal systems utilizing nanofluids. In spite of that, to the authors' knowledge, there is no specific review of the subject. Therefore, this is the aim in the present work. In the following section, researches on the nanoparticle shape considered by various researchers are presented. Afterwards, methods utilized for incorporating the effect of the shape of nanoparticle into the thermophysical properties of nanofluids are outlined. Thereafter, an overview of the published works on the effect of nanoparticle shape on the hydrothermal performance of thermal systems utilizing nanofluids is presented. The review covers forced, mixed, and natural convection regimes and includes boundary layer flows, channel flows, peristaltic flows, impinging jets, cavity flows, flows in heat exchangers, and flows of hybrid nanofluids. Finally, concluding remarks and future works are provided.

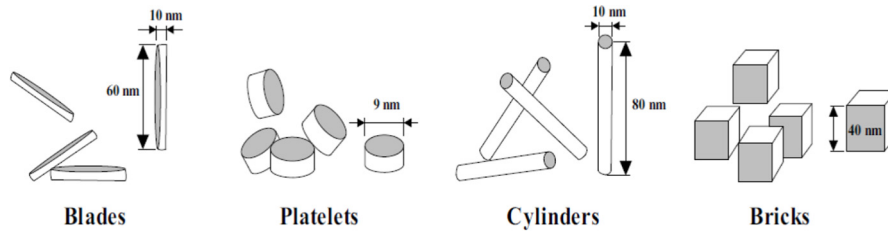
## 2. Nanoparticle shapes

Our literature survey demonstrates that various researchers considered brick, blade, platelet, cylindrical, spherical, oblate

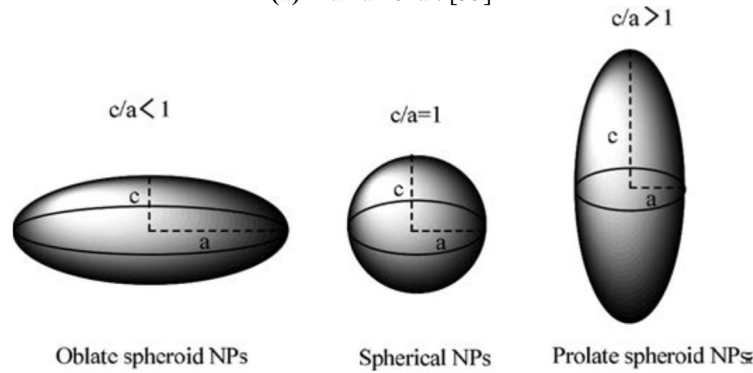
spheroid, prolate spheroid, hexahedron, tetrahedron, and lamina shapes for the nanoparticles suspended in different base fluids. Schematics of these shapes are shown in Fig. 2. Furthermore, SEM images of TiO<sub>2</sub> nanoparticles with several nanoparticle shapes are given in Fig. 3.

### 3. Models for the incorporation of the nanoparticle shape effect

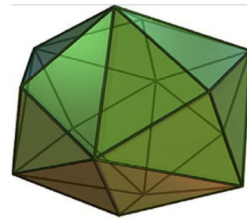
In this section, some well-known models utilized for the incorporation of the nanoparticle shape effect into the thermal conductivity and dynamic viscosity of nanofluids are presented.



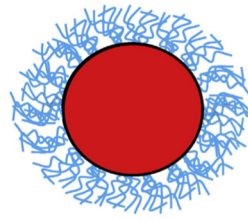
(a) Mahian et al. [33]



(b) Trodi and Benhamza [34]

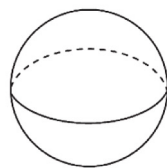


(c.1) Hexahedron

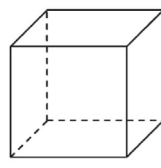


(c.2) Lamina

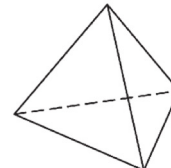
(c) Ghadikolaei and Gholinia [35]



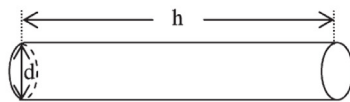
(a) Sphere



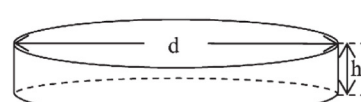
(b) Hexahedron



(c) Tetrahedron



(d) Column ( $h/d=20$ )



(e) Lamina ( $d/h=50$ )

(d) Lin et al. [36]

**Fig. 2.** Schematics of the nanoparticle shapes considered by various researchers. (Reprinted with permission from Elsevier and Taylor & Francis)

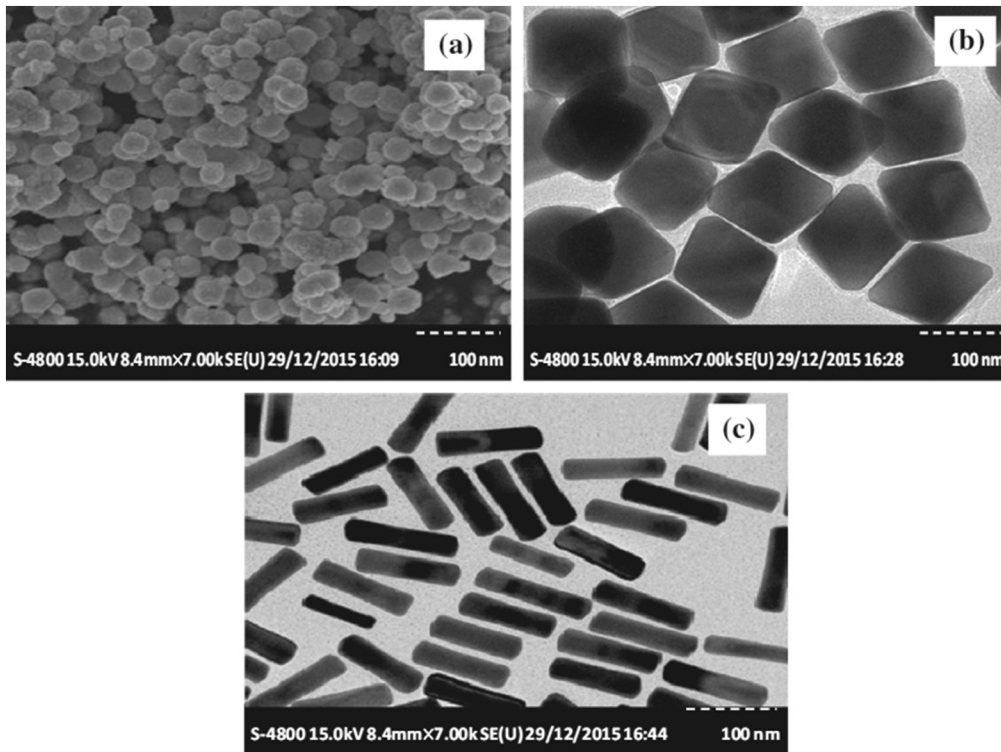


**Fig. 3.** SEM images of the  $\text{TiO}_2$  nanoparticles having (a) spherical, (b) brick (cubic), (c) cylindrical (rod) shapes [30]. (Reprinted with permission from Elsevier)

### 3.1. Thermal conductivity

Former researchers employed the Maxwell equation [37] for the evaluation of the thermal conductivity of nanofluids having spherical nanoparticles as:

$$k_{nf} = \frac{k_p + 2k_f - 2\phi(k_f - k_p)}{k_p + 2k_f + \phi(k_f - k_p)} k_f \quad (1)$$

Here,  $\phi$  is the volume fraction of the nanoparticles while  $k_f$  and  $k_p$  are thermal conductivities of the base fluid and the nanoparticles, respectively.

An alternative way has been the Koo–Kleinstreuer (K–K) model [38] with the form of:

$$k_{nf} = k_{st} + k_{Brwonian} \quad (2)$$

Here,  $k_{st}$  is the static part of thermal conductivity which is obtained through Eq. (1). Nevertheless, the second part stands for the contribution of Brownian motion on the thermal conductivity, which is given by:

$$k_{Brwonian} = 5 \times 10^4 \sigma \phi \rho_f C \sqrt{\frac{k_B T}{d_p \rho_p}} f(T, \phi) \quad (3)$$

with  $\sigma$  and  $f$  being empirical functions and  $k_B$  being the Boltzmann constant.

For nanofluids with non-spherical-shaped nanoparticles, some studies employed the Hamilton–Crosser (H–C) model [39], which is an extended Maxwell model as:

$$k_{nf} = \frac{k_p + (n-1)k_f - (n-1)\phi(k_f - k_p)}{k_p + (n-1)k_f + \phi(k_f - k_p)} k_f \quad (4)$$

Here,  $n$  is the empirical shape factor. This factor is defined as  $n = 3/\psi$  with  $\psi$  being sphericity, which is the ratio of the surface area of a similar-volume sphere to the surface area of the non-spherical-shaped nanoparticle. Table 1 reports the shape factor and sphericity of several

nanoparticle shapes. Note that by setting  $n = 3$  or  $\psi = 1$  (i.e., spherical-shaped nanoparticles), one arrives from the Hamilton–Crosser model to the Maxwell model.

An alternative way to incorporate the nanoparticle shape effect on thermal conductivity goes back to the use of the Timofeeva et al. [23] correlation for nanofluids containing different shapes of boehmite alumina nanoparticles dispersed in an ethylene glycol–water mixture (50:50) as:

$$k_{nf} = k_f \left[ 1 + \left( C_k^{shape} + C_k^{surface} \right) \phi \right] = k_f (1 + C_k \phi) \quad (5)$$

with  $C_k^{shape}$  standing for the role of nanoparticle shape on thermal conductivity (positive) and  $C_k^{surface}$  standing for the role of surface resistance to thermal conductivity (negative). Numerical values of  $C_k^{shape}$  and  $C_k^{surface}$  are reported in Table 2. The value of thermal conductivity of the ethylene glycol–water mixture at 25 °C is 0.3799 W/m.K [40].

### 3.2. Dynamic viscosity

The Brinkman model [41] was utilized by researchers to compute the dynamic viscosity of nanofluids having spherical-shaped nanoparticles as:

**Table 1**  
Shape factor and sphericity of several nanoparticle shapes.

Nanoparticle shape	Aspect ratio	Sphericity ( $\psi$ )	Shape factor ( $n$ )	Ref.
Brick	1:1:1	0.81	3.7	[40]
Blade	1:6:1/12	0.36	8.6	[40]
Platelet	1:1/8	0.52	5.7	[40]
Spherical	–	1	3	[40]
Cylindrical	1:8	0.62	4.9	[40]
Lamina	–	0.33	16.1576	[35]
Hexahedron	–	0.87	3.7221	[35]
Tetrahedron	–	0.25	4.0613	[36]



**Table 2**  
Constant coefficients in Eqs. (5) and (7).

Nanoparticle shape	$C_k^{shape}$	$C_k^{surface}$	$C_k$	$A_1$	$A_2$
Brick	3.72	−0.35	3.37	1.9	471.4
Blade	8.26	−5.52	2.74	14.6	123.3
Platelet	5.72	−3.11	2.61	37.1	612.6
Cylinder	4.82	−0.87	3.95	13.5	904.4

**Table 3**  
Thermal conductivity of the boehmite alumina nanofluid for different shapes of the nanoparticles based on the Timofeeva correlation.

Nanoparticle shape	Nanoparticles volume fraction				Rank
	0.005	0.01	0.015	0.02	
Brick	0.386	0.393	0.399	0.406	2
Blade	0.385	0.390	0.396	0.401	3
Platelet	0.385	0.390	0.395	0.400	4
Cylindrical	0.387	0.395	0.402	0.410	1

$$\mu_{nf} = \frac{\mu_f}{(1-\phi)^{2.5}} \quad (6)$$

For nanofluids having non-spherical-shaped boehmite alumina nanoparticles suspended in an ethylene glycol–water mixture (50:50), Timofeeva et al. [23] proposed the following viscosity correlation:

$$\mu_{nf} = \mu_f (1 + A_1\phi + A_2\phi^2) \quad (7)$$

The coefficients of  $A_1$  and  $A_2$  for different nanoparticle shapes are given in Table 2. The dynamic viscosity of the ethylene glycol–water mixture at 25 °C is 0.00339 kg/m.s.

### 3.3. Discussion

Thermal conductivity of several nanoparticle shapes obtained from the Timofeeva correlation (i.e., Eq. (5)) and the Hamilton–Crosser model are given in Tables 3 and 4, respectively, to provide a picture about the nanoparticle shape effect. Notice that both approaches predict that a rise in the nanoparticles volume fraction leads to thermal conductivity elevation, which is expected. Table 3 indicates that the Timofeeva correlation estimates that the highest values of thermal conductivity appear for the cylindrical nanoparticles while the lowest values occur for the platelet ones. Nevertheless, the results of the Hamilton–Crosser model are entirely different in both the thermal conductivity and the rank values. To demonstrate this effect further, percentages of deviation of the Hamilton–Crosser model from the Timofeeva correlation in the prediction of thermal conductivity of the boehmite alumina nanofluid are provided in Table 5. It is evident that the Hamilton–Crosser model predicts higher thermal conductivity values, especially for the blade and platelet nanoparticle shapes. The maximum discrepancy between the outcomes of these two approaches is about 10%. The observed

**Table 4**  
Thermal conductivity of the boehmite alumina nanofluid for different shapes of the nanoparticles based on the H–C model.

Nanoparticle shape	Nanoparticles volume fraction				Rank
	0.005	0.01	0.015	0.02	
Brick	0.387	0.393	0.400	0.407	4
Blade	0.395	0.410	0.425	0.440	1
Platelet	0.390	0.400	0.411	0.421	2
Spherical	0.385	0.391	0.397	0.402	5
Cylindrical	0.389	0.398	0.407	0.416	3

**Table 5**  
Percentages of deviation of the H–C model from the Timofeeva correlation in the prediction of the thermal conductivity of the boehmite alumina nanofluid.

Nanoparticle shape	Nanoparticles volume fraction			
	0.005	0.01	0.015	0.02
Brick	0.088	0.190	0.305	0.433
Blade	2.486	4.941	7.365	9.761
Platelet	1.346	2.682	4.009	5.327
Cylindrical	0.334	0.677	1.028	1.388

**Table 6**  
Dynamic viscosity of the boehmite alumina nanofluid for different shapes of the nanoparticles (the results of the spherical nanoparticles are based on the Brinkman model while the others are based on the Timofeeva correlation).

Nanoparticle shape	Nanoparticles volume fraction				Rank
	0.005	0.01	0.015	0.02	
Brick	0.00346	0.00362	0.00386	0.00417	4
Blade	0.00366	0.00394	0.00424	0.00456	3
Platelet	0.00408	0.00487	0.00576	0.00675	1
Spherical	0.00343	0.00348	0.00352	0.00357	5
Cylindrical	0.00370	0.00416	0.00478	0.00554	2

difference is attributed to the fact that the total surface area of the solid/liquid interface rises with an increase in the shape factor at a constant nanoparticles volume fraction [23]. This deteriorates the thermal conductivity enhancement due to the elevated surface resistance. However, this effect is ignored in the Hamilton–Crosser model. Therefore, the results of this model closely obey the shape factor values in such a way that a higher shape factor results in a higher thermal conductivity.

The numerical values of the dynamic viscosity of the boehmite alumina nanofluid for various nanoparticle shapes are reported in Table 6. Here, the viscosity values of the spherical nanoparticles are based on the Brinkman model while the others are based on the Timofeeva correlation (i.e., Eq. (7)). Notice the viscosity elevation due to the rise in the nanoparticles concentration in such a way that this elevation is faster for the non-spherical nanoparticles. The table shows that the highest and the lowest values of the nanofluid viscosity belong with the platelet and spherical nanoparticle shapes, respectively. In order to analyze this effect further, the percentages of deviation of the dynamic viscosity of the non-spherical nanoparticles from that of the spherical ones are listed in Table 7. The table indicates an elevation of up to about 90% for the dynamic viscosity of the non-spherical nanoparticles, as compared with the spherical ones. This indicates that the nanoparticle shape has prominent consequences on the viscosity of nanofluids. However, most of the researchers included the nanoparticle shape effect by changing the thermal conductivity through the Hamilton–Crosser model while ignoring the dependence of the fluid viscosity on the nanoparticle shape, which may not be valid.

Another shortcoming in the literature goes back to the fact that several authors employed the Timofeeva correlations proposed for the boehmite alumina nanofluid for the prediction of thermal conductivity and viscosity of other types of nanofluids, which is not accurate.

**Table 7**  
The percentages of deviation of dynamic viscosity of non-spherical nanoparticles from that of the spherical ones.

Nanoparticle shape	Nanoparticles volume fraction			
	0.005	0.01	0.015	0.02
Brick	0.842	4.214	9.507	16.890
Blade	6.519	13.225	20.335	27.827
Platelet	18.866	40.002	63.536	89.363
Cylindrical	7.908	19.785	35.705	55.505

#### 4. Nanoparticle shape effect in the forced convection regime

In this section, contributions relating to the nanoparticle shape effect on the forced convection regime are reviewed. The literature survey reveals that most of the previous works on the nanoparticle shape effect have been undertaken in this regime.

##### 4.1. Boundary layer flow

Lin et al. [36] examined nanoparticle shape effect on heat transfer of copper–water nanofluid during Marangoni boundary layer flow over an interface under the influence of gradient of surface tension. Comparison of the results of several shapes of the nanoparticles including sphere, hexahedron, tetrahedron, column, and lamina indicated that the spherical-shaped nanoparticles with low thermal conductivity had a better heat transfer elevation than other nanoparticles. Marangoni boundary layer flow of the suspension of different-shaped nanoparticles was also analyzed by Ellahi et al. [42] who compared the results of disk-shaped (platelet), needle-shaped (cylindrical), and spherical copper nanoparticles suspended in ethylene glycol.

Kandasamy et al. [43] investigated the effect of nanoparticle shape on squeezed nanofluid flow over a porous sensor surface under the influences of magnetic field and radiative heat exchange. Water, engine oil, and ethylene glycol were utilized as the base fluid while copper, alumina, and single-walled carbon nanotubes (SWCNTs) having lamina, cylindrical, or spherical shapes were employed for the nanoparticles. The spherical-shaped SWCNTs dispersed in engine oil had the most desirable heat transfer performance. In another attempt, Kandasamy et al. [44] employed these nanoparticle types and shapes suspended in water for MHD flow over a stretched surface. They led to the same conclusion regarding the shape of the nanoparticles.

Khan et al. [45] discussed MHD forced convection heat transfer of Cu–water nanofluid in a rotating stretching channel in the attendance of wall suction/blowing, radiative heat exchange, and viscous dissipation. The brick, platelet, and cylindrical-shaped nanoparticles were considered in this study. The three nanoparticle shapes led to almost the same skin friction coefficients but the platelet-shaped nanoparticles acquired the highest heat exchange rate.

Maraj et al. [46] assessed the hexahedron and lamina-shaped graphene oxide (GO) nanoparticles dispersed in ethylene glycol (EG) or propylene glycol (PG) in an MHD stagnation point flow over a stretching cylinder in the attendance of internal heat generation as well as thermal deposition. It was found that the shape of the nanoparticle played a vital role in the heat transfer mechanism. The highest Nusselt number was observed for the lamina-shaped nanoparticles dispersed in EG.

Shaiq et al. [47] evaluated the role of the nanoparticle shape factor on an MHD stagnation point flow towards a stretching cylinder for titanium dioxide or copper nanoparticles dispersed in ethylene glycol. Brick, blade, platelet, and cylindrical nanoparticles were utilized for this aim. The strong dependence of the heat transfer rate on the shape and size of the nanoparticles was clarified during this investigation. The outcomes showed that the blade-shaped copper nanoparticles led to the highest temperature. These nanoparticles also produced the maximum values of surface heat flux. Additionally, the skin friction was higher for the copper nanoparticles than for the titanium dioxide ones.

Ganesh et al. [48] investigated fluid dynamics and heat transfer in Blasius and Sakiadis slip flows of boehmite alumina nanoparticles with various shapes (brick, blade, platelet, cylindrical, and spherical) suspended in an ethylene glycol–water mixture. Excluding the spherical-shaped nanoparticles, direct relation was reported between the Nusselt number and the nanoparticle loading.

In another study, Saleem et al. [49] focused on heat transfer improvement using different shapes of copper nanoparticles in the boundary layer flow of a water-based nanofluid over a flat surface. To this aim,

blade, platelet, and spherical nanoparticle shapes were analyzed. Results showed that the nanoparticle shape affected the skin friction and the Nusselt number, substantially. The platelet-shaped nanoparticles contributed to the maximum rise in velocity and temperature and the most considerable improvement in heat transfer.

Kumar et al. [50] explored the effect of nanoparticle shape on hydrodynamics and heat transfer of Cu–water nanofluid over a moving plate. They observed that among the disk-shaped (platelet), needle-shaped (cylindrical), and spherical nanoparticles, the highest temperature level appeared for the disk-shaped ones.

##### 4.2. Channel flow

Arani et al. [51] evaluated the nanoparticle shape effect on the hydrothermal performance of turbulent nanofluid flow through a wavy minichannel. The nanofluid was made up of boehmite alumina nanoparticles suspended in an ethylene glycol–water mixture with brick, blade, platelet, cylindrical, spherical, oblate spheroidal, and prolate spheroidal nanoparticle shapes. Outcomes are displayed in Fig. 4. A comparison of the cylindrical, brick, blade, platelet, and spherical nanoparticles indicated that the brick-shaped nanoparticles contributed to the highest heat transfer rate. Nevertheless, nanofluid containing the blade-shaped nanoparticles had the lowest friction factor. In terms of PEC (Performance Evaluation Criteria), however, the brick-shaped nanoparticles exhibited the best overall performance. They also determined optimum configurations for the oblate spheroidal and prolate spheroidal nanoparticle shapes and compared these responses with the outcomes of the pure base fluid as well as the blade-shaped and the spherical-shaped nanoparticles. It was concluded that the addition of the non-spherical nanoparticles to a base fluid could not improve the hydrothermal performance of the minichannel.

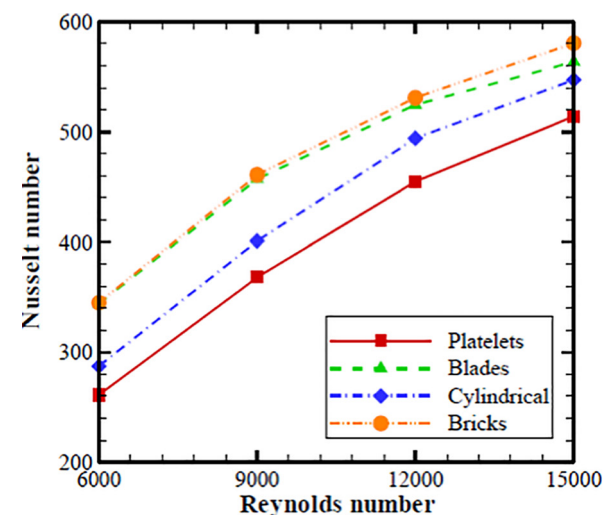
A similar study, but in the laminar flow regime was undertaken by Vo et al. [52]. They compared the outcomes of the brick, blade, platelet, and cylindrical-shaped nanoparticles. However, they reported that the platelet-shaped nanoparticles led to the highest heat transfer rate. The lowest pressure drop also appeared in the nanofluid containing the brick-shaped nanoparticles. Moreover, in terms of PEC, the platelet-shaped nanoparticles achieved the best overall performance.

Nguyen et al. [53] examined the effect of shape of copper oxide nanoparticles suspended in water on laminar flow of nanofluid through a sinusoidal channel with obstacles. To this aim, they considered brick, platelet, cylindrical, and spherical nanoparticle shapes. The heat transfer rate was improved more than 55% when they replaced the spherical nanoparticles with the platelet ones.

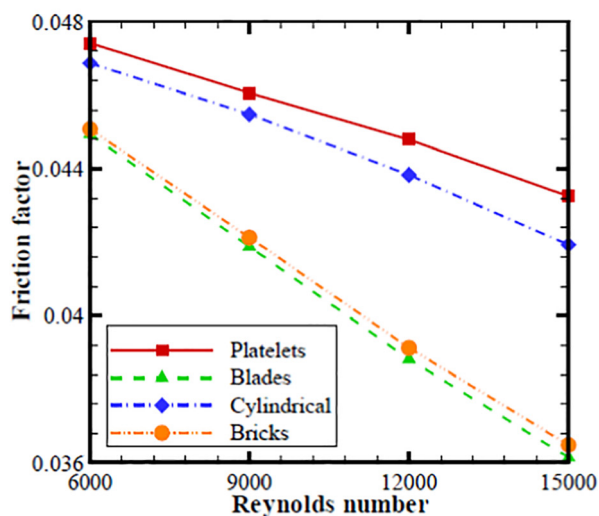
Khan et al. [54] discussed MHD flow and heat transfer of copper–water nanofluid through a parallel-plates channel for several nanoparticle shapes (i.e., brick, platelet, and cylindrical). In this study, the shape of the nanoparticles had no significant effect on the velocity distribution but it affected the temperature profile substantially. The platelet-shaped nanoparticles maximized the temperature level but the brick-shaped nanoparticles minimized it. The highest heat transfer rate was detected in a fluid containing the platelet-shaped nanoparticles.

Nanoparticle shape effect on molybdenum disulfide–water nanofluid during an unsteady MHD channel flow in the attendance of radiative heat exchange as well as wall suction/blowing was clarified by Raza et al. [55]. Accordingly, lamina, cylindrical, and spherical nanoparticles were analyzed. The outcomes demonstrated that the spherical nanoparticles elevated the heat transfer rate more than the other ones.

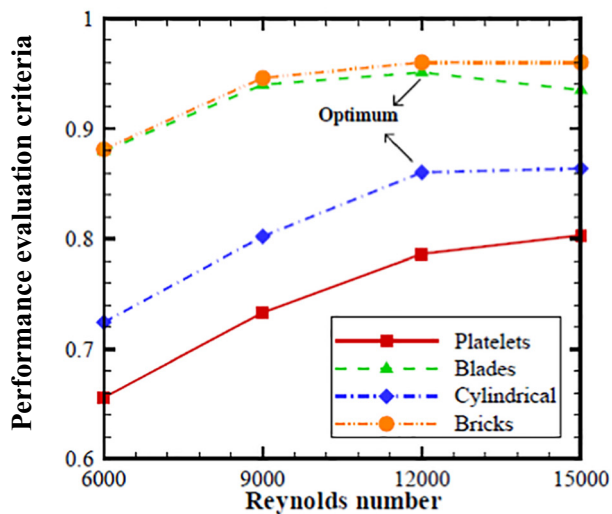
Gireesha et al. [56] simulated the slip flow of nanofluids through a microchannel in the attendance of internal heat generation, convective boundary conditions, and various shapes of nanoparticles. The nanofluid was MoS<sub>2</sub> or TiO<sub>2</sub> nanoparticles suspended in water. They reported that the blade-shaped nanoparticles boosted the heat exchange more than the brick, platelet, cylindrical, and spherical ones. Furthermore, their entropy generation investigation revealed that the highest entropy generation rate belonged to the spherical nanoparticles.



(a) Mean Nusselt number



(b) Friction factor



(c) Performance evaluation criteria

Bahiraee et al. [57] assessed the nanoparticle shape effect on entropy generation during turbulent flow and heat transfer of boehmite alumina–water nanofluid through a channel having conical ribs. To this aim, they considered brick, blade, platelet, cylindrical, and oblate spheroid nanoparticle shapes. It was shown that the platelet-shaped nanoparticles led to the lowest value of the total entropy generation rate.

#### 4.3. Impinging jets

Selimfendigil and Öztöp [58] discussed how the nanoparticle shape might alter the heat removal from a corrugated plate cooled with an impinging jet of a SiO<sub>2</sub>–water nanofluid. Inspection of the results of the brick, blade, cylindrical, and spherical nanoparticle shapes showed that the cylindrical-shaped nanoparticles offered the highest values of the stagnation and mean Nusselt numbers. They found that for the spherical-shaped nanoparticles, the Nusselt number was a linear function of the nanoparticles volume fraction. However, deviations from linearity were reported when the cylindrical-shaped nanoparticles were employed.

Nimmagadda et al. [59] analyzed the nanoparticle shape effect on the hydrodynamics and heat transfer of MHD jet impingement over a stationary/vibrating plate. To this aim, they considered several shapes of carbon nanoparticles, which included nanotubes, nanorods, and nanosheets. At the nanoparticle volume fraction of 3%, the percentage enhancements in the average Nusselt number with the nanotubes, nanorods, and nanosheets were recorded to be 26.85, 26.86, and 47.53, as compared with the pure water.

#### 4.4. Cavity flow

Sheikholeslami and Rokni [60] and Nguyen et al. [61] simulated the hydrodynamics and heat transfer of Fe<sub>3</sub>O<sub>4</sub>–ethylene glycol nanofluid in lid-driven porous cavities under the influence of Coulomb force. The brick, platelet, cylindrical, and spherical nanoparticle shapes were concerned. The maximum heat transfer rate was reported for the platelet-shaped nanoparticles.

#### 4.5. Flow in heat exchangers

Elias et al. [40] studied analytically the effect of nanoparticle shape on heat transfer as well as entropy generation in a shell and tube heat exchanger. The analysis was conducted for an ethylene glycol–water mixture containing brick, blade, platelet, cylindrical, or spherical shapes of boehmite alumina nanoparticles. The best heat transfer performance appeared for the cylindrical-shaped nanoparticles followed by the bricks, blades, platelets, and spherical ones. Meanwhile, entropy generation of a nanofluid containing the cylindrical-shaped nanoparticles was just about 1% higher than the other nanoparticle shapes. Thereby, the cylindrical-shaped nanoparticles were recommended to elevate the overall performance of the heat exchanger. In another attempt, Elias et al. [62] extended their work to a shell and tube heat exchanger having baffles, which led to the same conclusions regarding the nanoparticle shape.

Mahian et al. [33] reported first and second laws analysis for the effect of nanoparticle shape and tube material on a minichannel-based solar collector, working with a suspension of boehmite alumina nanoparticles in ethylene glycol–water mixture. Several nanoparticle shapes (brick, blade, platelet, and cylindrical) and two materials for the tubes and the absorber plate (copper and steel) were examined. As indicated in Fig. 5, excluding the highest volume fraction (i.e., 4%), the brick-shaped nanoparticles displayed the highest Nusselt number. Moreover,

Fig. 4. Effect of nanoparticle shape on the outcomes of Arani et al. [51] for the nanoparticle volume fraction of 4%. (Reprinted with permission from Elsevier)



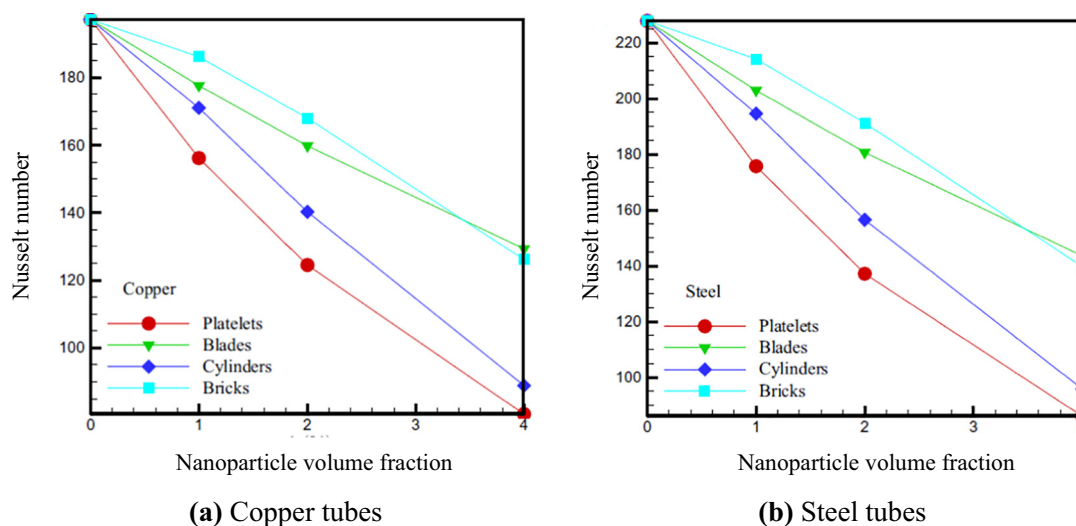


Fig. 5. Effect of nanoparticle shape as well as tubes materials on the outcomes of Mahian et al. [33] for  $m = 0.75$  kg/s. (Reprinted with permission from Elsevier)

the Nusselt number for the steel tubes was higher than that of the copper ones. The undertook second law analysis for the copper tubes revealed that when one utilized the brick-shaped nanoparticles with the volume fraction of 2%, the entropy generation rate was minimized. For the steel tubes, however, the minimum entropy generation rate was attained for the blade-shaped nanoparticles with the nanoparticle volume fraction of 4%.

Shahsavari et al. [63] undertook a hydrothermal analysis of laminar nanofluid flow in a double-pipe minichannel heat exchanger. Boehmite alumina nanoparticles with brick, blade, platelet, cylindrical, or spherical shapes suspended in a mixture of water–ethylene glycol was chosen as the nanofluid. Outcomes are displayed in Fig. 6. Notice that the platelet-shaped nanoparticles and the spherical-shaped nanoparticles represented the maximum and the minimum values of both heat transfer rate and pumping power, respectively. However, in terms of the performance index, the spherical-shaped nanoparticles offered the best overall performance. Alsarraf et al. [64] extended this work to the turbulent flow regime. As depicted in Fig. 6, they reached similar conclusions regarding the nanoparticle shape effect (Fig. 7).

In another attempt, Al-Rashed et al. [65] discussed how nanoparticle shape might affect entropy generation rate in laminar nanofluid flow through a double-pipe minichannel heat exchanger. As shown in Fig. 8, nanofluids having the platelet-shaped nanoparticles and the spherical-shaped nanoparticles had the highest and lowest rates of entropy generation, respectively. More precisely, the rate of entropy generation for a nanofluid having the platelet-shaped nanoparticles was up to about 519.16% higher than that containing the spherical-shaped nanoparticles. Meanwhile, the highest Bejan number (i.e., the ratio of heat transfer irreversibility to total global entropy generation rate [66]) was reported for the platelet-shaped nanoparticles. An extension of this work to the turbulent flow regime was provided by Monfared et al. [67]. Conversely, they reported the highest and lowest rates of entropy generation for the spherical-shaped nanoparticles and the platelet-shaped nanoparticles, respectively. Moreover, the maximum value of the Bejan number was associated with the nanofluids having the spherical-shaped nanoparticles (see Fig. 9).

Sadripour and Chamkha [68] compared heat transfer and entropy generation of nanofluids made up of different shapes of copper (Cu), silver (Ag), alumina ( $\text{Al}_2\text{O}_3$ ), boehmite alumina ( $\gamma\text{-AlOOH}$ ), molybdenum disulfide ( $\text{MoS}_2$ ), and silicon dioxide ( $\text{SiO}_2$ ) nanoparticles in a water-based heat sink solar collector. Regarding the heat transfer, the spherical-shaped nanoparticles displayed the best performance both for the metallic and non-metallic nanoparticles. However, the

minimum entropy generation rate was achieved for the spherical shapes and the brick shapes in the metallic and non-metallic nanoparticles, respectively.

Liu et al. [69] simulated heat transfer, entropy generation, and heat flow path of CuO–water nanofluid in a finned multi-pipe heat exchanger. They focused on exploring the effect of nanoparticle shape on the simulation results by comparing the outcomes of cylindrical, platelet, brick, and spherical-shaped nanoparticles. The platelet-shaped nanoparticles acquired the best heat transfer performance.

Bahiraie and Monavari [70] performed a hydrothermal analysis of a micro plate heat exchanger operating with nanofluid as the hot fluid and pure water as the cold fluid. The nanofluid was made up of an ethylene glycol–water mixture containing brick, blade, platelet, cylindrical, or oblate spheroid shapes of boehmite alumina nanoparticles. The platelet-shaped nanoparticles and the oblate spheroid nanoparticles showed the highest and lowest values of heat transfer rate, respectively. In spite of that, the oblate spheroid nanoparticles caused the lowest pressure drop and the highest performance index.

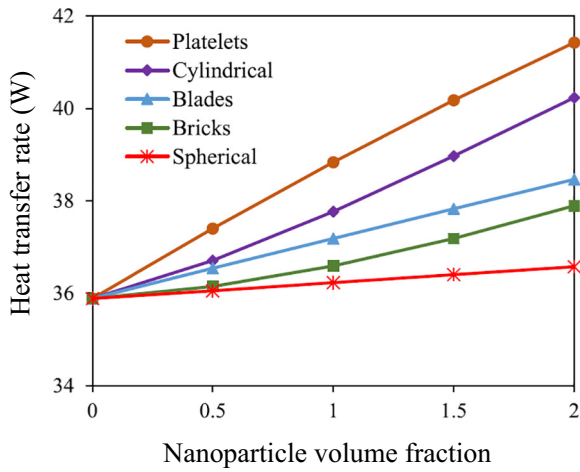
## 5. Nanoparticle shape effect in the mixed convection regime

Several types of research were performed to explore the nanoparticle shape effect on mixed convection heat transfer, which are reviewed in this section.

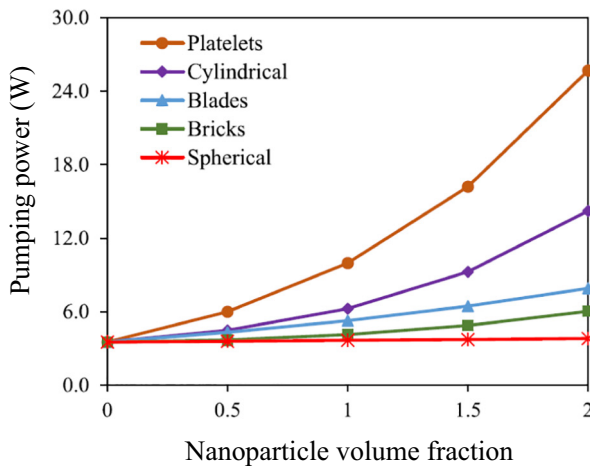
### 5.1. Peristaltic flow

Akbar and Butt [71] obtained the exact solution for MHD mixed convection in the peristaltic flow of copper–water nanofluid for cases having a low Reynolds number and long wavelength. Thereafter, they compared the outcomes of brick, platelet, and cylindrical nanoparticle shapes. Scrutiny of their results indicated that changing the nanoparticles from bricks to cylinders or platelets raised the temperature. The highest pressure gradient was found in the platelet-shaped nanoparticles.

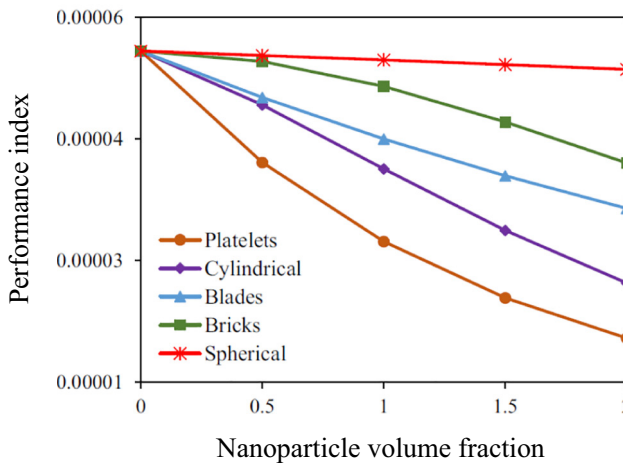
Akbar et al. extended their work to incorporate flow unsteadiness [72] and magnetic field insertion [73]. Both studies demonstrated that the platelet-shaped nanoparticles acquired the highest velocity. In the attendance of the magnetic field (i.e., [73]), maximum values of temperature and pressure gradient were associated with the shape of brick, which was in contrast with what they observed in its absence (i.e., [71]).



(a) Heat transfer rate



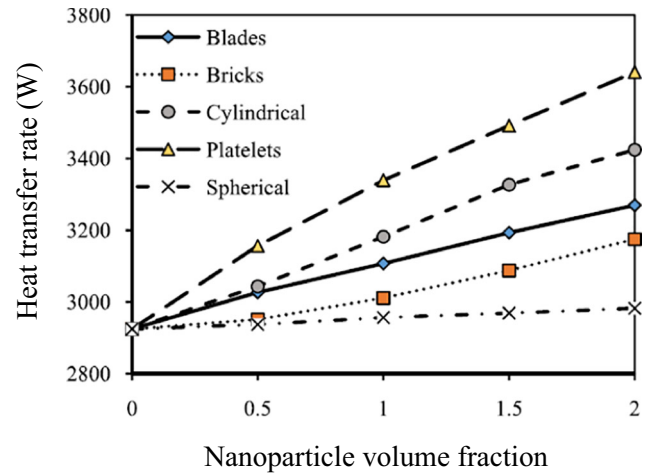
(b) Required pumping power



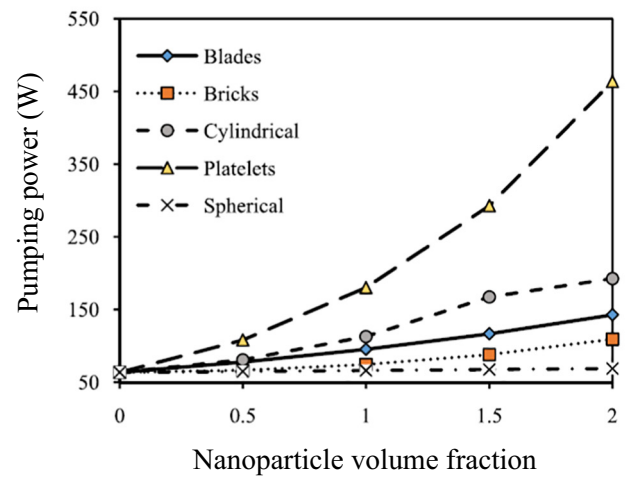
(c) Performance index

Fig. 6. Effect of nanoparticle shape on the outcomes of Shahsavari et al. [63] at  $Re = 2000$ . (Reprinted with permission from Springer)

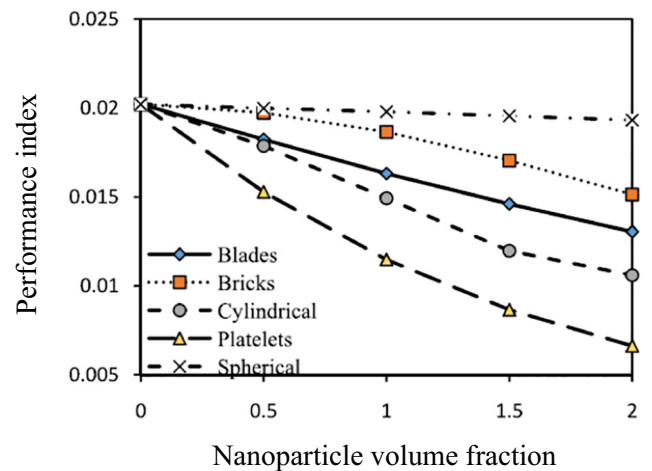
In a recent investigation, the consequences of nanoparticle shape on MHD mixed convection during peristaltic flow in an asymmetric channel were discussed by Khan et al. [74], who compared the results of the disk (blade), cylindrical, and spherical nanoparticles.



(a) Heat transfer rate

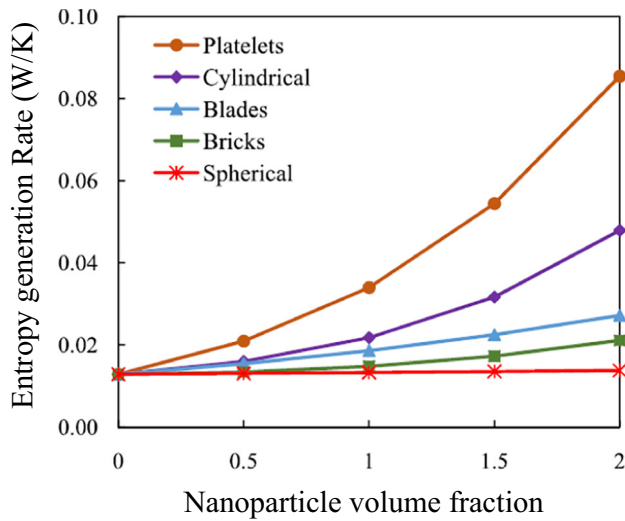


(b) Required pumping power

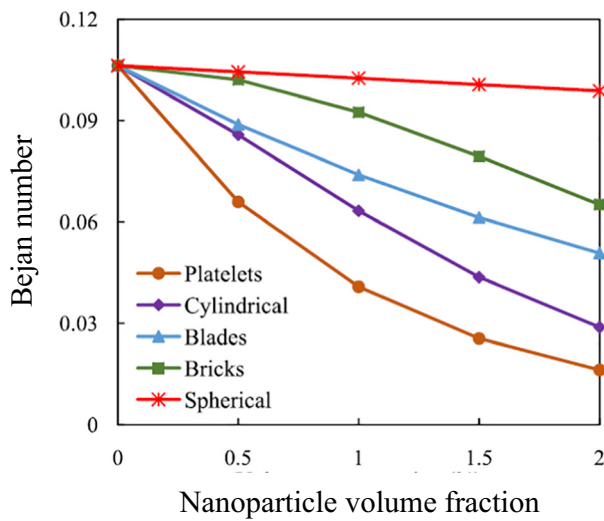


(c) Performance index

Fig. 7. Effect of nanoparticle shape on the outcomes of Alsaarraf et al. [64] at  $Re = 20,000$ . (Reprinted with permission from Elsevier)



(a) Entropy generation rate



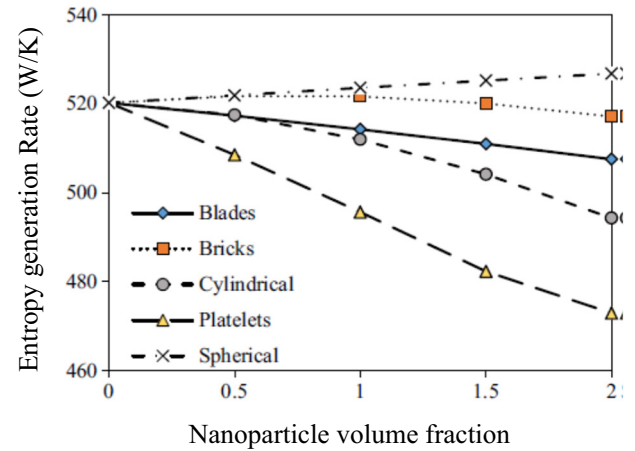
(b) Bejan number

Fig. 8. Effect of nanoparticle shape on the outcomes of Al-Rashed et al. [65] at  $Re = 2000$ . (Reprinted with permission from Elsevier)

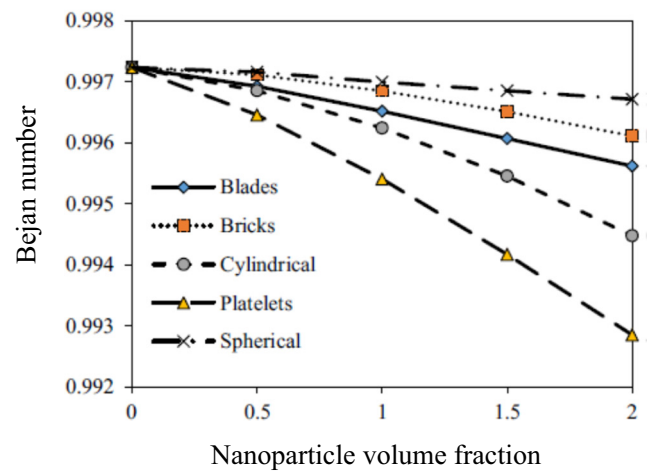
### 5.2. Boundary layer flow

Ellahi et al. [75] studied the shape effect of Nimonic 80a nanoparticles suspended in HFE (Human Engineered Fluid) in mixed convection over a wedge within a porous medium. The analysis was undertaken for the needle-shaped (cylindrical), disk-shaped (blade), and spherical nanoparticles. The highest values of temperature, velocity, and entropy generation rate were reported for the disk-shaped, spherical, and needle-shaped nanoparticles, respectively. It was reported that the non-spherical shaped nanoparticles were more stimulated for heat transfer enhancement.

Zeeshan et al. [76] employed different shapes of nanoparticles in an unsteady mixed convection of nanofluid over a rotating disk. For the nanofluid, copper nanoparticles with the disk (blade), cylindrical, or spherical shapes suspended in water were considered. Scrutiny of the outcomes demonstrated that the spherical-shaped nanoparticles gained the maximum fluid temperature. However, nanofluid having the cylindrical-shaped nanoparticles offered the highest velocity. The maximum irreversibility was found for the disk-shaped nanoparticles, followed by the cylindrical and spherical shapes.



(a) Entropy generation rate



(b) Bejan number

Fig. 9. Effect of nanoparticle shape on the outcomes of Monfared et al. [67] at  $Re = 20,000$ . (Reprinted with permission from Springer)

Ellahi et al. [77] discussed the nanoparticle shape effect on mixed convection heat transfer of Nimonic 80a–HFE nanofluid over a vertical stretching permeable plate. Comparison of the results of the needle-shaped (cylindrical), the disk-shaped (blade), and the spherical-shaped nanoparticles led to the conclusion that the lowest values of temperature and wall shear stress occurred for the needle-shaped nanoparticles.

Mahanthesh et al. [78] focused on the effect of nanoparticle shape on unsteady mixed convection heat transfer of nanofluids over a rotating plate in the attendance of Hall current, chemical reaction, porous medium, and temperature-dependent heat generation. Copper, copper oxide, aluminum, alumina, and titanium oxide nanoparticles having column, lamina, tetrahedron, hexahedron, or spherical shapes suspended in blood, ethylene glycol, engine oil, or glycerin were considered as the nanofluid. Among the 20 nanofluids analyzed, the Cu–EG nanofluid achieved the highest heat transfer rate. Furthermore, the temperature level of the lamina-shaped nanoparticles was largest.

Izadi et al. [79] analyzed MHD mixed convection heat transfer of a micropolar nanofluid over a stretching plate within a porous medium. The nanofluid had a magnetic field-dependent viscosity, which was made up of copper nanoparticles dispersed in water. The brick, platelet, cylindrical, and spherical nanoparticle shapes were concerned and the corresponding results were compared. The results showed that the

maximum and minimum values of both temperature and velocity appeared in the fluid containing the spherical and platelet nanoparticles, respectively.

### 5.3. Cavity flow

Selimefendigil et al. [80] focused on mixed convection heat transfer occurring as a result of rotation of a cylinder inside a flexible-wall cavity filled with  $\text{SiO}_2$ -water nanofluid in the attendance of heat generation. They considered several nanoparticle shapes including brick, blade, spherical, and cylindrical. Among them, the cylindrical nanoparticles and the spherical ones exhibited the best and the worst performance for heat transfer enhancement, respectively.

In another attempt, Selimefendigil et al. [81] simulated MHD mixed convection of  $\text{SiO}_2$ -water nanofluid in a cubic cavity having a conductive partition for several nanoparticle shapes (i.e., blade, brick, spherical, and cylindrical). The blade-shaped nanoparticles exhibited the worst heat transfer performance while the cylindrical-shaped ones exhibited the best heat transfer performance. However, the results of these nanoparticle shapes in terms of the mean Nusselt number were less than 3% apart.

### 5.4. Other flow problems

Khan [82] discussed the shape effect of  $\text{MoS}_2$  nanoparticles suspended in water on MHD mixed convection through a vertical porous channel in the slip flow regime. Molybdenum disulfide nanoparticles were utilized in different shapes including brick, blade, cylindrical, platelet, and spherical. Inspection of the results showed that nanoparticles having the blade shape led to the highest heat transfer rate. The heat transfer rate of nanofluids containing the blade, platelet, cylindrical, brick, and spherical nanoparticle shapes were found 8.1, 5.7, 4.7, 3.7, and 2.9% higher than the base fluid, respectively.

Ijaz et al. [83] studied the importance of nanoparticle shape on electro-osmosis mixed convection of nanofluid in a curved channel. To this aim, alumina-water nanofluid with blade, brick, platelet, and cylindrical-shaped nanoparticles was considered. The best thermal performance was recorded for the blade-shaped nanoparticles.

## 6. Nanoparticle shape effect in the natural convection regime

In the literature, several studies were reported relating the nanoparticle shape effect on natural convection heat transfer as follows.

### 6.1. Boundary layer flow

Zaraki et al. [84] focused on the consequence of size, shape, and type of nanoparticles as well as the type of base fluid and temperature level on natural convection boundary layer heat and mass transfer of nanofluids. Regarding the nanoparticle geometry, they compared the rectangular and spherical shapes of  $\text{ZnO}$  nanoparticles. It was found that the maximum velocity of the nanofluid having the spherical nanoparticles was slightly higher than that the velocity of the rectangular nanoparticles. The temperature profiles were, however, almost identical. The nearly negligible effect of the nanoparticle shape on the heat transfer improvement was also observed in the analysis of Sabour et al. [85], who discussed similar parameters but for cavity flows.

Ghadikolaei and Gholinia [35] simulated three-dimensional MHD natural convection of nanofluids over a porous vertical stretching plate under the influences of radiative heat exchange and suction/blowing. The nanofluid was produced by suspending copper nanoparticles in the hexahedron or lamina shapes within an ethylene glycol-water hybrid base fluid. It was noticed that the lamina-shaped nanoparticles had a more significant effect on elevating temperature and the heat transfer rate compared with that of the hexahedron ones.

### 6.2. Cavity flow

Paul et al. [86] performed an experimental study on natural convection heat transfer of a nanoparticle enhanced ionic liquid (NEIL) in rectangular cavities. They synthesized the NEIL by dispersing alumina nanoparticles with spherical or whisker shapes into an ionic liquid. The whisker-shaped nanoparticles had slightly higher Nusselt number than the spherical-shaped nanoparticles.

Shirvan et al. [87] analyzed the consequences of nanoparticle shape on natural convection heat transfer as well as entropy generation characteristics of nanofluids in a wavy-wall cavity through response surface methodology. The blade, cylindrical, and spherical nanoparticles were compared. The highest values of heat exchange and entropy generation rate were recorded for the spherical-shaped nanoparticles.

Trodi and Benhamza [34] focused on the roles of nanoparticle shape and aspect ratio of alumina-water nanofluid on natural convection in a square cavity. Three different nanoparticle shapes (spherical, oblate spheroid, and prolate spheroid) with several aspect ratios were compared. The nanoparticle shape and aspect ratio possessed prominent consequences on the natural convection heat transfer. The oblate spheroid nanoparticles offered the largest enhancement in the heat transfer. For the prolate spheroids, direct relation was reported between the heat transfer rate and the nanoparticle aspect ratio.

Sheikhzadeh et al. [88] discussed the effect of nanoparticle shape on natural convection heat transfer of  $\text{SiO}_2$ -water nanofluid in a partitioned square cavity. They utilized the nanoparticles having brick, blade, platelet, cylindrical, or spherical shapes. It was observed that when  $10^3 < Ra < 10^5$ , the nanoparticle shape produced minor consequences on the heat transfer rate. However, for higher values of the Rayleigh number, the nanoparticle shape effect became evident in such a way that the platelet-shaped nanoparticles acquired the highest Nusselt number.

Alkanhal et al. [89] compared the results of brick, platelet, cylindrical, and spherical nanoparticles suspended in water in MHD natural convection heat transfer within a wavy-wall porous cavity having a square obstacle and a radiative heat source. The highest Nusselt number occurred in the fluid containing the blade-shaped nanoparticles.

Dogonchi et al. [90] studied the shape effect of  $\text{CuO}$  nanoparticles on natural convection heat transfer in a partially-heated rhombus cavity having a circular barrier at its center. They considered the cylindrical, platelet, and spherical nanoparticle shapes. It was noticed that the heat transfer rate reached its maximum value when using the platelet-shaped nanoparticles. The minimum heat transfer rate belonged to the spherical-shaped nanoparticles. Similar outcomes were obtained when they extended their work to incorporate the magnetic field insertion [91].

Rahimi et al. [92] focused on natural convection heat transfer in a finned/multi-pipe cavity filled with  $\text{CuO}$ -water nanofluid. They examined the consequences of the nanoparticle shape on the simulation results. The brick, platelet, cylindrical, and spherical-shaped nanoparticles were considered. The most proper nanoparticles in terms of heat transfer improvement were platelet-shaped.

Nguyen et al. [93] employed a two-temperature model to simulate MHD natural convection of copper oxide-water nanofluid flow in a permeable cavity. They compared the results of brick, platelet, cylindrical, and spherical nanoparticle shapes. The best nanoparticles were the platelet-shaped ones.

The consequence of nanoparticle shape on MHD natural convection of copper-water nanofluid in an irregular triangular cavity was discussed by Dogonchi et al. [94]. They compared the results of platelets, cylindrical, and spherical nanoparticles and noticed that the nanoparticle shape factor possessed prominent consequences on the heat transfer rate in such a way that the shape factor elevation improved the heat transfer rate. Therefore, the platelet-shaped nanoparticles exhibited the highest heat transfer rate.

Shahsavari et al. [95] analyzed how the nanoparticle shape may affect natural convection and entropy generation in a finned concentric horizontal annular cavity filled with nanofluid. The nanofluid was made



up of brick, blade, platelet, cylindrical, or spherical-shaped boehmite alumina nanoparticles dispersed in a 50:50 mixture of ethylene glycol and water. The cylindrical and platelet-shaped nanoparticles acquired the best performances regarding the first and the second laws of thermodynamics, respectively.

Gholinia et al. [96] compared the outcomes of the tetrahedron, cylindrical, and spherical CuO nanoparticles in MHD natural convection of binary-based nanofluids (ethylene glycol–water mixture) within a porous cavity in the attendance of radiative heat exchange. The cylindrical-shaped nanoparticles demonstrated a greater effect on heat transfer enhancement compared with the other shapes.

In another attempt, Gholinia et al. [97] simulated natural convection within an intricate-shaped porous cavity and compared the heat transfer performance of brick, platelet, lamina, and tetrahedron TiO<sub>2</sub> nanoparticles suspended in an ethylene glycol–water mixture. The highest Nusselt number was recorded for the lamina-shaped nanoparticles.

Shape effectiveness of alumina nanoparticles on the MHD natural convection heat transfer in a porous cavity was discussed by Vo et al. [98]. To this aim, outcomes were presented for the brick, platelet, cylindrical, and spherical-shaped nanoparticles. Inspection of the results indicated that a direct relation existed between the nanoparticle shape factor and the heat transfer rate in such a way that the platelet-shaped nanoparticles acquired the best performance.

### 6.3. Other flow problems

KhakRah et al. [99] considered the brick, platelet, cylindrical, and spherical-shaped nanoparticles for natural convection of CuO–water nanofluid in a  $\Gamma$ -shaped heat exchanger. Among them, the platelet-shaped nanoparticles led to the highest heat transfer augmentation.

Sowmya et al. [100] studied thermal behavior of a radial porous fin wetted with a suspension produced by dispersing brick, blade, platelet, or cylindrical shapes of molybdenum disulfide nanoparticles within water. The brick-shaped nanoparticles yielded the highest heat transfer performance compared with the other shapes.

## 7. Nanoparticle shape effect in hybrid nanofluids

Some researchers discussed the nanoparticle shape effect on the flows of hybrid nanofluids. Examples in the forced, mixed, and natural convection regimes are discussed in the following.

### 7.1. Forced convection regime

Ghadikolaei et al. [101] compared the results of brick, platelet, and cylindrical-shaped TiO<sub>2</sub>–Cu hybrid nanoparticles dispersed in water in an MHD stagnation point flow over a horizontal stretching plate. The highest heat transfer rate was reported for the platelet-shaped nanoparticles.

Ghadikolaei et al. [102] analyzed the effect of the nanoparticle shape factor on three-dimensional squeezing flow of hybrid nanoparticles (Fe<sub>3</sub>O<sub>4</sub>–Ag) dispersed in a binary base fluid (ethylene glycol–water). Accordingly, three shapes of nanoparticles including brick, platelet, and cylindrical were utilized. They noticed that raising the shape factor reduced the temperature level but elevated the heat transfer rate. Therefore, the highest heat transfer rate was reported for the platelet-shaped nanoparticles with the highest value of the shape factor.

Dinarvand et al. [103] investigated how nanoparticle shape in TiO<sub>2</sub>/CuO–water hybrid nanofluid may alter fluid flow and heat transfer over a static/moving wedge or corner. The platelet-shaped nanoparticles led to the highest local Nusselt number in comparison with other shapes including brick, cylindrical, and spherical.

Bhatta and Sarkar [104] assessed the effect of the shape and size of hybrid nanoparticles on the hydrothermal performance of a plate evaporator using nanofluids. Water-based solutions of ethylene glycol (EG), propylene glycol (PG), calcium chloride (CaCl<sub>2</sub>), and potassium acetate

(KAC) were utilized as the base fluid while the hybrid nanoparticles were considered as combinations of copper oxide, alumina, titania, or silica with copper nanoparticles. The PG and EG-based Cu–CuO hybrid nanofluids gave the highest heat transfer rates while the Cu–SiO<sub>2</sub> hybrid nanoparticles performed well in terms of the exergetic efficiency. Among the brick, platelet, cylindrical, and spherical nanoparticles, the brick-shaped ones showed the maximum alternation in the performance index while the platelet-shaped ones led to the worst performance.

Benkhedda et al. [105] considered the nanoparticle shape effect on the heat transfer performance of hybrid nanofluids flowing through a tube. The tube was filled with water, TiO<sub>2</sub>–water nanofluid, or Ag/TiO<sub>2</sub>–water hybrid nanofluid. Four different types of nanoparticle shapes were considered which include platelet, blade, cylindrical, and spherical. The highest heat transfer rate belonged to the blade-like nanoparticles followed by the platelet, cylindrical, and spherical ones. In addition, the highest friction factor was reported for the platelet-shaped nanoparticles.

Ghobadi and Hassankolaei [106] studied the role of nanoparticle shape on MHD convection heat transfer of Al<sub>2</sub>O<sub>3</sub>/TiO<sub>2</sub>–H<sub>2</sub>O hybrid nanofluids over a stretching cylinder in the presence of heat generation and nonlinear thermal radiation. They compared the hexahedron and lamina-shaped nanoparticles and found that changing the hexahedron nanoparticles to the lamina ones elevated the temperature level. Moreover, the lamina-shaped nanoparticles were more influential on the Nusselt number.

Aziz et al. [107] focused on heat transfer as well as entropy generation of Maxwell hybrid nanofluid over a porous stretching disk in the attendance of inclined magnetic field, Joule heating, radiative heat exchange, and nanoparticle shape factor. Comparison of the results of Cu/EG and Fe<sub>3</sub>O<sub>4</sub>–Cu/EG nanofluids showed higher heat transfer performance for the hybrid nanoparticles. Meanwhile, inverse relation was recorded between the heat transfer rate and the nanoparticle shape factor.

### 7.2. Mixed convection regime

Ghadikolaei et al. [108] examined the effect of shape factor on MHD non-Newtonian hybrid nanofluid flow and heat transfer over a rotating cone under the influence of buoyancy force, heat generation/absorption, radiative heat exchange, and variable thermal conductivity. The nanofluid was a suspension of TiO<sub>2</sub> and CuO hybrid nanoparticles in an ethylene glycol–water mixture with the brick, blade, cylindrical, or platelet-shaped nanoparticles. They reported that raising the shape factor elevated the temperature level as well as the Nusselt number. Therefore, the blade-shaped nanoparticles had the highest heat transfer rate. It was also noticed that the hybrid nanoparticles produced more prominent consequences on temperature distribution than the single nanoparticles. Similar conclusions were drawn when Ghadikolaei and Gholinia [109] studied three-dimensional MHD mixed convection of GO–MoS<sub>2</sub> nanoparticles dispersed in an ethylene glycol–water mixture in the attendance of radiative heat exchange, slip factor, and shape factor.

Maraj et al. [110] presented a shape effect investigation for MHD flow and heat transfer of MoS<sub>2</sub>–SiO<sub>2</sub>/H<sub>2</sub>O nanofluid in a semi-vertical inverted cone with porous wall in the attendance of viscous dissipation and radiative heat exchange. The highest and the lowest values of the skin friction coefficient and the Nusselt number were reported for the blade and brick-shaped nanoparticles, respectively.

### 7.3. Natural convection regime

Ghadikolaei et al. [111] simulated three-dimensional MHD natural convection of nanofluid over a vertical stretching plate under the effect of variable thermal conductivity, radiative heat exchange, and the nanoparticle shape factor. The nanofluid consisted of MoS<sub>2</sub>–Ag hybrid nanoparticles suspended in an ethylene glycol–water mixture. They considered the brick, blade, platelet, and cylindrical nanoparticle shapes. The hybrid nanoparticles led to higher values of heat

transfer rate and thermal boundary layer thickness, as compared with the single ones. Shape factor showed an incremental consequence on the temperature profile as well as the Nusselt number in such a way that the blade-shaped nanoparticles had the highest values of the Nusselt number.

Sahu et al. [112] conducted both energetic and exergetic analysis for a natural circulation loop operating with water-based hybrid nanofluids. To this aim,  $\text{Al}_2\text{O}_3$ -Ag,  $\text{Al}_2\text{O}_3$ -CNT,  $\text{Al}_2\text{O}_3$ - $\text{TiO}_2$ ,  $\text{Al}_2\text{O}_3$ -CuO,  $\text{Al}_2\text{O}_3$ -Cu, and  $\text{Al}_2\text{O}_3$ -GNPs hybrid nanoparticles having platelet, cylindrical, or spherical-shapes were considered. The nanoparticle shape had prominent consequences on the performance of the system. The hybrid nanofluids having platelet-shaped GNPs yielded the lowest mass flow rate compared with the other nanofluids, which was attributed to an enormous rise in the dynamic viscosity.

## 8. Discussion

The presented literature survey indicated that there was no uniform conclusion on the effect of nanoparticle shape on the hydrothermal performance of thermal systems. In this section, we try to collect the outcomes of the previous studies to determine statistically how each of the mentioned nanoparticle shapes has led to the highest heat transfer performance in different flow regimes. To this aim, Fig. 10 is plotted. Notice in Fig. 10(a) that in about 42% of the previous studies in the forced convection regime, the platelet-shaped nanoparticle acquired the highest heat transfer rate. The second and the third nanoparticles were spherical and cylindrical, respectively. The trend in the natural convection regime (i.e., Fig. 10(c)) is similar. However, about 35% of the previous studies in this flow regime have reported the platelet shape as the optimum nanoparticle shape for heat transfer enhancement. Inspection of Fig. 10(b) and (d) demonstrates that in the mixed convection regime as well as the flow of hybrid nanofluids, the blade-shaped nanoparticle led to the best heat transfer performance. This is in contrast with what we observed in the natural and forced convection regimes and reveals that the role of nanoparticle shape on the heat transfer elevation is dependent to the regime of the flow.

## 9. Concluding remarks and future works

This paper offered an overview of the nanoparticle shape effect on the hydrothermal performance of thermal systems utilizing nanofluids. The conclusions and future research directions of this review are as follows:

- (1) To include the nanoparticle shape effect, both thermal conductivity and dynamic viscosity of the nanofluid must be modified.
- (2) Incorporation of the nanoparticle shape effect with alternation of thermal conductivity through the Hamilton-Crosser model may not be accurate.
- (3) Identifying a suitable nanoparticle shape for each system could effectively improve its hydrothermal performance and decrease its entropy generation rate.
- (4) There is no uniform conclusion on the role of nanoparticle shape on the hydrothermal performance of thermal systems.
- (5) The effect of nanoparticle shape on the heat transfer enhancement is dependent to the regime of the flow.
- (6) In most of the previous studies in the natural and forced convection regimes, the platelet-like nanoparticle led to the best heat transfer performance. However, most of the works in the mixed convection regime reported the highest heat transfer rate for the blade-like nanoparticle.
- (7) Future researches should further strengthen the studies on fluid dynamics and heat transfer of different shapes of nanoparticles.
- (8) Most of the efforts on the nanoparticle shape effect on the hydrothermal performance of thermal systems are theoretical through incorporating it in thermophysical properties while experimental verification is relatively lacking. Hence, future experimental measurements are required for different nanoparticle shapes in various nanofluids having single and hybrid nanoparticles.

## Declaration of competing interest

We declare that we have no financial and personal relationships with other people or organizations that can inappropriately influence

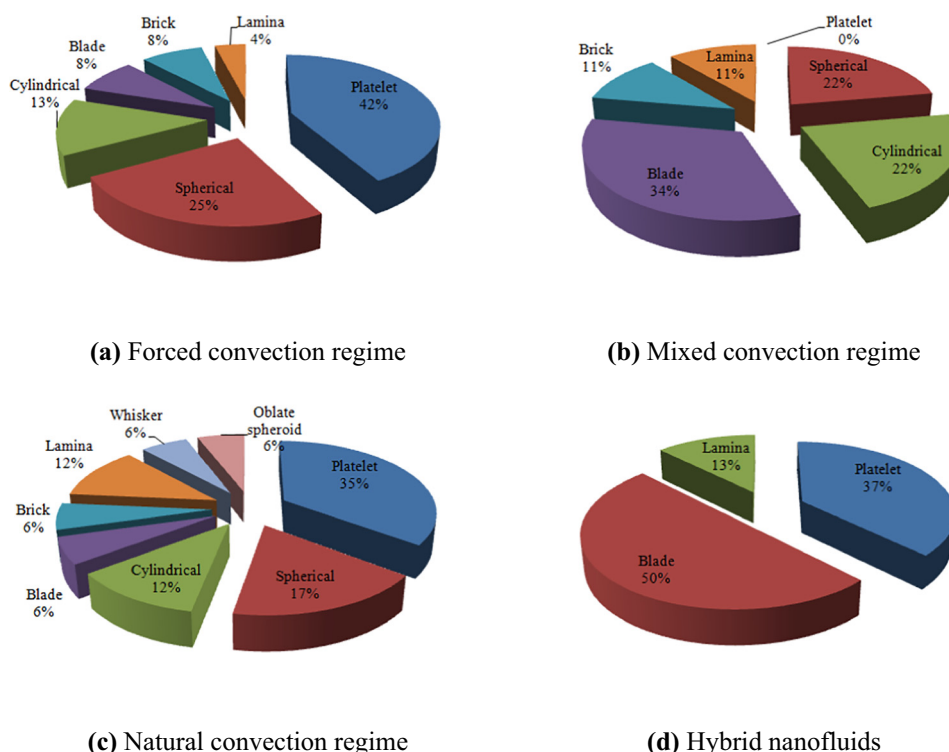


Fig. 10. Statistical illustration of the optimum nanoparticle shape for heat transfer enhancement in previous studies.

our work, there is no professional or other personal interest of any nature or kind in any product, service and/or company that could be construed as influencing the position presented in, or the review of, the manuscript entitled.

## Acknowledgements

The authors gratefully acknowledge the financial support of the National Natural Science Foundation of China (No. 51776165) and the financial support from Royal Society–Newton Advanced Fellowship grant (NAF/R1/191163). The eighth author acknowledges the support provided by the NSTDA Research Chair Grant.

## References

- [1] O. Mahian, L. Kolsi, M. Amani, P. Estellé, G. Ahmadi, C. Kleinstreuer, J.S. Marshall, M. Siavashi, R.A. Taylor, H. Niazmand, S. Wongwises, T. Hayat, A. Kolarjijil, A. Kasaeian, I. Pop, Recent advances in modeling and simulation of nanofluid flows—part I: fundamental and theory, *Phys. Rep.* 790 (2019) 1–48.
- [2] O. Mahian, L. Kolsi, M. Amani, P. Estelle, G. Ahmadi, C. Kleinstreuer, J.S. Marshall, R.A. Taylor, E. Abu-Nada, S. Rashidi, H. Niazmand, S. Wongwises, T. Hayat, A. Kasaeian, I. Pop, Recent advances in modeling and simulation of nanofluid flows—part II: applications, *Phys. Rep.* 791 (2019) 1–59.
- [3] T.C. Paul, A.K.M.M. Morshed, J.A. Khan, Effect of nanoparticle dispersion on thermophysical properties of ionic liquids for its potential application in solar collector, *Procedia Engineering* 90 (2014) 643–648.
- [4] I. Zahmatkesh, On the suitability of volume-averaging approximation for the description of thermal expansion coefficient of nanofluids, *Proc. Inst. Mech. Eng. C J. Mech. Eng. Sci.* 229 (2015) 2835–2841.
- [5] M.H. Esfe, M. Goodarzi, M. Reiszadeh, M. Afrand, Evaluation of MWCNTs–ZnO/5W50 nanolubricant by design of an artificial neural network for predicting viscosity and its optimization, *J. Mol. Liq.* 277 (2019) 921–931.
- [6] A. Ghaffarkhah, M. Afrand, M. Talebkeikhah, A.A. Sehat, M.K. Moraveji, F. Talebkeikhah, M. Arjmand, On evaluation of thermophysical properties of alumina–MWCNTs/salt-water nanofluids: a comprehensive modeling and experimental study, *J. Mol. Liq.* 300 (2020), 112249.
- [7] A. Dadwal, P.A. Joy, Particle size effect in different base fluids on the thermal conductivity of fatty acid coated magnetite nanofluids, *J. Mol. Liq.* 303 (2020), 112650.
- [8] A.H. Sharifi, I. Zahmatkesh, F.F. Bamoharram, A.H.S. Tabrizi, S.F. Razavi, S. Saneinezhad, Experimental measurement of thermophysical properties of alumina–MWCNTs/salt-water hybrid nanofluids, *Curr. Nanosci.* 16 (2020) 734–747.
- [9] A.H. Sharifi, I. Zahmatkesh, A.M. Mozhdehi, A. Morsali, F.F. Bamoharram, Stability appraisalment of the alumina–brine nanofluid in the presence of ionic and non-ionic disperse on the alumina nanoparticles surface as heat transfer fluids: quantum mechanical study and Taguchi–optimized experimental analysis, *J. Mol. Liq.* 319 (2020), 113898.
- [10] T.C. Paul, R. Mahamud, J.A. Khan, Multiphase modeling approach for ionic liquids (ILs) based nanofluids: improving the performance of heat transfer fluids (HTFs), *Appl. Therm. Eng.* 149 (2019) 165–172.
- [11] B. Bakthavatchalam, K. Habib, R. Saidur, B.B. Saha, K. Irshad, Comprehensive study on nanofluid and ionanofluid for heat transfer enhancement: a review on current and future perspective, *J. Mol. Liq.* 305 (2020), 112787.
- [12] M. Ghalandari, A. Maleki, A. Haghighi, M.S. Shadloo, M.A. Nazari, I. Tlili, Applications of nanofluids containing carbon nanotubes in solar energy systems: a review, *J. Mol. Liq.* 313 (2020) 113476.
- [13] F. Abbas, H.M. Ali, T.R. Shah, H. Babar, M.M. Janjua, U. Sajjad, M. Amer, Nanofluid: potential evaluation in automotive radiator, *J. Mol. Liq.* 297 (2020), 112014.
- [14] M. Ghalambaz, S.A.M. Mehryan, I. Zahmatkesh, A. Chamkha, Free convection heat transfer analysis of a suspension of nano-encapsulated phase change materials (NEPCMs) in an inclined porous cavity, *Int. J. Therm. Sci.* 157 (2020), 106503.
- [15] I. Zahmatkesh, S.A. Naghedifar, Oscillatory mixed convection in jet impingement cooling of a horizontal surface immersed in a nanofluid–saturated porous medium, *Numerical Heat Transfer, Part A* 72 (2017) 401–416.
- [16] I. Zahmatkesh, M.R.H. Shandiz, Optimum constituents for MHD heat transfer of nanofluids within porous cavities: a Taguchi analysis in natural and mixed convection configurations, *J. Therm. Anal. Calorim.* 138 (2019) 1669–1681.
- [17] I. Zahmatkesh, E. Torshizi, Scrutiny of unsteady flow and heat transfer in a backward-facing step under pulsating nanofluid blowing using the Eulerian–Eulerian approach, *J. Mech.* 35 (2019) 93–105.
- [18] I. Zahmatkesh, M.R. Habibi, Natural and mixed convection of nanofluid in porous cavities: critical analysis using the Buongiorno's model, *J. Theor. Appl. Mech.* 57 (2019) 221–233.
- [19] M.R. Habibi, I. Zahmatkesh, Double-diffusive natural and mixed convection of binary nanofluids in porous cavities, *Journal of Porous Media* 23 (2020) 955–967.
- [20] S.S. Bazkhan, I. Zahmatkesh, Taguchi-based sensitivity analysis of hydrodynamics and heat transfer of nanofluids in a microchannel heat sink (MCHS) having porous substrates, *International Communications in Heat and Mass Transfer* 118 (2020) 104885.
- [21] H. Xie, J. Wang, T. Xi, Y. Liu, Thermal conductivity of suspensions containing nanosized SiC particles, *Int. J. Thermophys.* 23 (2002) 571–580.
- [22] S.M.S. Murshed, K.C. Leong, C. Yang, Enhanced thermal conductivity of TiO<sub>2</sub>–water based nanofluids, *Int. J. Therm. Sci.* 44 (2005) 367–373.
- [23] E.V. Timofeeva, J.L. Routbort, D. Singh, Particle shape effects on thermophysical properties of alumina nanofluids, *J. Appl. Phys.* 106 (2009), 014304.
- [24] D. Singh, E. Timofeeva, W. Yu, J. Routbort, D. France, D. Smith, J.L. Cepero, An investigation of silicon carbide–water nanofluid for heat transfer applications, *J. Appl. Phys.* 105 (2009) 064306.
- [25] J. Jeong, C. Li, Y. Kwon, J. Lee, S.H. Kim, R. Yun, Particle shape effect on the viscosity and thermal conductivity of ZnO nanofluids, *Int. J. Refrig.* 36 (2013) 2233–2241.
- [26] Z.T. Yu, X. Fang, L.W. Fan, X. Wang, Y.Q. Xiao, Y. Zeng, X. Xu, Y.C. Hu, K.F. Cen, Increased thermal conductivity of liquid paraffin–based suspensions in the presence of carbon nano-additives of various sizes and shapes, *Carbon* 53 (2013) 277–285.
- [27] X. Fang, Q. Ding, L.W. Fan, Z.T. Yu, X. Xu, G.H. Cheng, Y.C. Hu, K.F. Cen, Thermal conductivity enhancement of ethylene glycol–based suspensions in the presence of silver nanoparticles of various shapes, *J. Heat Transf.* 136 (2014) 034501.
- [28] H.J. Kim, S.H. Lee, J.H. Lee, S.P. Jang, Effect of particle shape on suspension stability and thermal conductivities of water–based boehmite alumina nanofluids, *Energy* 90 (2015) 1290–1297.
- [29] P.B. Maheshwary, C.C. Handa, K.R. Nemade, A comprehensive study of effect of concentration, particle size and particle shape on thermal conductivity of titania/water based nanofluid, *Appl. Therm. Eng.* 119 (2017) 79–88.
- [30] P.B. Maheshwary, C.C. Handa, K.R. Nemade, S.R. Chaudhary, Role of nanoparticle shape in enhancing the thermal conductivity of nanofluids, *Materials Today: Proceedings* 28 (2020) 873–878.
- [31] L. Zhang, W. Yu, D. Zhu, H. Xie, G. Huang, Enhanced thermal conductivity for nanofluids containing silver nanowires with different shapes, *J. Nanomater.* (2017) 5802016.
- [32] U. Nithiyantham, L. González-Fernández, Y. Grosu, A. Zaki, J.M. Igartua, A. Faik, Shape effect of Al<sub>2</sub>O<sub>3</sub> nanoparticles on the thermophysical properties and viscosity of molten salt nanofluids for TES application at CSP plants, *Appl. Therm. Eng.* 169 (2020), 114942.
- [33] O. Mahian, A. Kianifar, S.Z. Heris, S. Wongwises, First and second laws analysis of a minichannel–based solar collector using boehmite alumina nanofluids: effects of nanoparticle shape and tube materials, *Int. J. Heat Mass Transf.* 78 (2014) 1166–1176.
- [34] A. Trodi, M.E.H. Benhamza, Particle shape and aspect ratio effect of Al<sub>2</sub>O<sub>3</sub>–water nanofluid on natural convective heat transfer enhancement in differentially heated square enclosures, *Chem. Eng. Commun.* 204 (2017) 158–167.
- [35] S.S. Ghadikolaei, M. Gholinia, Terrific effect of H<sub>2</sub> on 3D free convection MHD flow of C<sub>2</sub>H<sub>6</sub>O<sub>2</sub>–H<sub>2</sub>O hybrid base fluid to dissolve Cu nanoparticles in a porous space considering the thermal radiation and nanoparticle shapes effects, *Int. J. Hydrog. Energy* 44 (2019) 17072–17083.
- [36] Y. Lin, B. Li, L. Zheng, G. Chen, Particle shape and radiation effects on Marangoni boundary layer flow and heat transfer of copper–water nanofluid driven by an exponential temperature, *Powder Technol.* 301 (2016) 379–386.
- [37] J.C. Maxwell, A Treatise on Electricity and Magnetism: Unabridged, Dover, 1954.
- [38] J. Koo, C. Kleinstreuer, Laminar nanofluid flow in microheat–sinks, *Int. J. Heat Mass Transf.* 48 (2005) 2652–2661.
- [39] R. Hamilton, O. Crosser, Thermal conductivity of heterogeneous two-component systems, *Ind. Eng. Chem. Fundam.* 1 (1962) 187–191.
- [40] M.M. Elias, M. Miqdad, I.M. Mahbubul, R. Saidur, M. Kamalifarvestani, M.R. Sohel, A. Hepbasli, N.A. Rahim, M.A. Amalina, Effect of nanoparticle shape on the heat transfer and thermodynamic performance of a shell and tube heat exchanger, *International Communications in Heat and Mass Transfer* 44 (2013) 93–99.
- [41] H.C. Brinkman, The viscosity of concentrated suspensions and solutions, *J. Chem. Phys.* 20 (1952) 571.
- [42] R. Ellahi, A. Zeeshan, M. Hassan, Particle shape effects on Marangoni convection boundary layer flow of a nanofluid, *International Journal of Numerical Methods for Heat & Fluid Flow* 26 (2016) 2160–2174.
- [43] R. Kandasamy, R. Mohammad, N.A.B.M. Zailani, N.F.B. Jaafar, Nanoparticle shapes on squeezed MHD nanofluid flow over a porous sensor surface, *J. Mol. Liq.* 233 (2017) 156–165.
- [44] R. Kandasamy, R. Dharmalingam, K.K.S. Prabhu, Lorentz forces and nanoparticle shape on water based Cu, Al<sub>2</sub>O<sub>3</sub> and SWCNTs, *J. Mol. Liq.* 231 (2017) 663–672.
- [45] U. Khan, A. Abbas, N. Ahmed, S.T. Mohyud-Din, Particle shape, thermal radiation, viscous dissipation and Joule heating effects on flow of magneto–nanofluid in a rotating system, *Eng. Comput.* 34 (2017) 2479–2498.
- [46] E.N. Maraj, S. Shaiq, Z. Iqbal, Assessment of hexahedron and lamina shaped graphene oxide nanoparticles suspended in ethylene and propylene glycol influenced by internal heat generation and thermal deposition, *J. Mol. Liq.* 262 (2018) 275–284.
- [47] S. Shaiq, E. Maraj, Z. Iqbal, A comparative analysis of shape factor and thermophysical properties of electrically conducting nanofluids TiO<sub>2</sub>–EG and Cu–EG towards stretching cylinder, *Chaos, Solitons Fractals* 118 (2019) 290–299.
- [48] N.V. Ganesh, Q.M. Al-Mdallal, K. Reena, S. Aman, Blasius and Sakiadis slip flow of H<sub>2</sub>O–C<sub>2</sub>H<sub>6</sub>O<sub>2</sub> (50:50) based nanoliquid with different geometry of boehmite alumina nanoparticles, *Case Studies in Thermal Engineering* 16 (2019), 100546.
- [49] S. Saleem, M. Qasim, A. Alderremy, S. Noreen, Heat transfer enhancement using different shapes of Cu nanoparticles in the flow of water based nanofluid, *Phys. Scr.* 95 (2020), 055209.
- [50] K.G. Kumar, A.J. Chamkha, B.C. Prasannakumara, A.M. Jyothi, Exploration of particle shape effect on Cu–H<sub>2</sub>O nanoparticles over a moving plate: an approach of dual solution, *International Journal of Numerical Methods for Heat & Fluid Flow* 30 (2019) 1867–1879.
- [51] A.A.A. Arani, S. Sadripour, S. Kermani, Nanoparticle shape effects on thermal–hydraulic performance of boehmite alumina nanofluids in a sinusoidal–wavy mini–channel with phase shift and variable wavelength, *Int. J. Mech. Sci.* 128–129 (2017) 550–563.
- [52] D.D. Vo, J. Alsaarraf, A. Moradikazerouni, M. Afrand, H. Salehipour, C. Qi, Numerical investigation of  $\gamma$ -AIOOH nano-fluid convection performance in a wavy channel



- considering various shapes of nanoadditives, *Powder Technol.* 345 (2019) 649–657.
- [53] T.K. Nguyen, A. Saidizad, M. Jafaryard, M. Sheikholeslami, M.B. Gerdroodbarye, R. Moradif, A. Shafeeg, Z. Lih, Influence of various shapes of CuO nanomaterial on nanofluid forced convection within a sinusoidal channel with obstacles, *Chem. Eng. Res. Des.* 146 (2019) 478–485.
- [54] U. Khan, N. Ahmed, S.T. Mohyud-Din, Analysis of magnetohydrodynamic flow and heat transfer of Cu–water nanofluid between parallel plates for different shapes of nanoparticles, *Neural Comput. Applic.* 29 (2018) 695–703.
- [55] J. Raza, F. Mebarek-Oudina, A.J. Chamkha, Magnetohydrodynamic flow of molybdenum disulfide nanofluid in a channel with shape effects, *Multidiscip. Model. Mater. Struct.* 15 (2019) 737–757.
- [56] B.J. Gireesha, S. Sindhu, Entropy generation analysis of nanofluid flow through microchannel considering heat source and different shapes of nanoparticle, *International Journal of Numerical Methods for Heat & Fluid Flow* 30 (2019) 1457–1477.
- [57] M. Bahraei, A. Monavari, H. Moayed, Second law assessment of nanofluid flow in a channel fitted with conical ribs for utilization in solar thermal applications: effect of nanoparticle shape, *Int. J. Heat Mass Transf.* 151 (2020), 119387.
- [58] F. Selimefendigil, H.F. Öztop, Effects of nanoparticle shape on slot jet impingement cooling of a corrugated surface with nanofluids, *Journal of Thermal Science and Engineering Applications* 9 (2017), 021016.
- [59] R. Nimmagadda, G.A. Lazarus, S. Wongwises, Effect of magnetic field and nanoparticle shape on jet impingement over stationary and vibrating plates, *International Journal of Numerical Methods for Heat & Fluid Flow* 29 (2019) 4948–4970.
- [60] M. Sheikholeslami, H.B. Rokni, Numerical simulation for impact of Coulomb force on nanofluid heat transfer in a porous enclosure in presence of thermal radiation, *Int. J. Heat Mass Transf.* 118 (2018) 823–831.
- [61] T.K. Nguyen, F.A. Soomro, J.A. Ali, R.U. Haq, M. Sheikholeslami, A. Shafee, Heat transfer of ethylene glycol–Fe<sub>3</sub>O<sub>4</sub> nanofluid enclosed by curved porous cavity including electric field, *Physica A* 550 (2020), 123945.
- [62] M.M. Elias, I.M. Shahrlul, I.M. Mahbubul, R. Saidur, N.A. Rahim, Effect of different nanoparticle shapes on shell and tube heat exchanger using different baffle angles and operated with nanofluid, *Int. J. Heat Mass Transf.* 70 (2014) 289–297.
- [63] A. Shahsavari, Z. Rahimi, H. Salehipour, Nanoparticle shape effects on thermal-hydraulic performance of boehmite alumina nanofluid in a horizontal double-pipe minichannel heat exchanger, *Heat Mass Transf.* 55 (2019) 1741–1751.
- [64] J. Alsarraf, A. Moradikazerouni, A. Shahsavari, M. Afrand, H. Salehipour, M.D. Tran, Hydrothermal analysis of turbulent boehmite alumina nanofluid flow with different nanoparticle shapes in a minichannel heat exchanger using two-phase mixture model, *Physica A* 520 (2019) 275–288.
- [65] A.A.A.A. Al-Rashed, R. Ranjbarzadeh, S. Aghakhani, M. Soltanimehr, M. Afrand, T.K. Nguyen, Entropy generation of boehmite alumina nanofluid flow through a minichannel heat exchanger considering nanoparticle shape effect, *Physica A* 521 (2019) 724–736.
- [66] I. Zahmatkesh, On the importance of thermal boundary conditions in heat transfer and entropy generation for natural convection inside a porous enclosure, *Int. J. Therm. Sci.* 47 (2008) 339–346.
- [67] M. Monfared, A. Shahsavari, M.R. Bahrebar, Second law analysis of turbulent convection flow of boehmite alumina nanofluid inside a double-pipe heat exchanger considering various shapes for nanoparticle, *J. Therm. Anal. Calorim.* 135 (2019) 1521–1532.
- [68] S. Sadripour, A.J. Chamkha, The effect of nanoparticle morphology on heat transfer and entropy generation of supported nanofluids in a heat sink solar collector, *Thermal Science and Engineering Progress* 9 (2019) 266–280.
- [69] J.B. Liu, M. Bayati, M. Abbas, A. Rahimi, M. Naderi, Mesoscopic approach for simulating nanofluid flow and heat transfer in a finned multi-pipe heat exchanger, *International Journal of Numerical Methods for Heat & Fluid Flow* 29 (2019) 2822–2839.
- [70] M. Bahraei, A. Monavari, Thermohydraulic characteristics of a micro plate heat exchanger operated with nanofluid considering different nanoparticle shapes, *Appl. Therm. Eng.* 179 (2020) 11562.
- [71] N.S. Akbar, A.W. Butt, Ferromagnetic effects for peristaltic flow of Cu–water nanofluid for different shapes of nanosize particles, *Appl. Nanosci.* 6 (2016) 379–385.
- [72] N.S. Akbar, A.W. Butt, D. Tripathi, Nanoparticle shapes effects on unsteady physiological transport of nanofluids through a finite length non-uniform channel, *Results in Physics* 7 (2017) 2477–2484.
- [73] N.S. Akbar, A.B. Huda, M.B. Habib, D. Tripathi, Nanoparticles shape effects on peristaltic transport of nanofluids in presence of magnetohydrodynamics, *Microsyst. Technol.* 25 (2019) 283–294.
- [74] L.A. Khan, M. Raza, N.A. Mir, R. Ellahi, Effects of different shapes of nanoparticles on peristaltic flow of MHD nanofluids filled in an asymmetric channel: a novel model for heat transfer enhancement, *J. Therm. Anal. Calorim.* 140 (2020) 879–890.
- [75] R. Ellahi, M. Hassan, A. Zeeshan, A.A. Khan, The shape effects of nanoparticles suspended in HFE-7100 over wedge with entropy generation and mixed convection, *Appl. Nanosci.* 6 (2016) 641–651.
- [76] A. Zeeshan, M. Hassan, R. Ellahi, M. Nawaz, Shape effect of nanosize particles in unsteady mixed convection flow of nanofluid over disk with entropy generation, *Proceedings of the Institution of Mechanical Engineers, Part E: J Process Mechanical Engineering* 231 (2017) 871–879.
- [77] R. Ellahi, M. Hassan, A. Zeeshan, Shape effects of spherical and non-spherical nanoparticles in mixed convection flow over a vertical stretching permeable sheet, *Mech. Adv. Mater. Struct.* 24 (2017) 1231–1238.
- [78] B. Mahanthesh, S. Amala, B.J. Gireesha, I.L. Animasaun, Effectiveness of exponential heat source, nanoparticle shape factor and Hall current on mixed convective flow of nanofluids subject to rotating frame, *Multidiscip. Model. Mater. Struct.* 15 (2019) 758–778.
- [79] M. Izadi, M. Javanahram, S.M. Hashem Zadeh, D. Jing, Hydrodynamic and heat transfer properties of magnetic fluid in porous medium considering nanoparticle shapes and magnetic field-dependent viscosity, *Chin. J. Chem. Eng.* 28 (2020) 329–339.
- [80] F. Selimefendigil, H.F. Öztop, N. Abu-Hamdeh, Mixed convection due to rotating cylinder in an internally heated and flexible walled cavity filled with SiO<sub>2</sub>–water nanofluids: effect of nanoparticle shape, *International Communications in Heat and Mass Transfer* 71 (2016) 9–19.
- [81] F. Selimefendigil, H.F. Öztop, A.J. Chamkha, MHD mixed convection of nanofluid in a cubic cavity with a conductive partition for various nanoparticle shapes, *International Journal of Numerical Methods for Heat & Fluid Flow* 29 (2019) 3584–3610.
- [82] I. Khan, Shape effects of MoS<sub>2</sub> nanopartilces on MHD slip flow of molybdenum disulphide nanofluid in a porous medium, *J. Mol. Liq.* 233 (2017) 442–451.
- [83] N. Ijaz, A. Zeeshan, S.U. Rehman, Effect of electro-osmosis and mixed convection on nano-bio-fluid with non-spherical particles in a curved channel, *Mechanics & Industry* 19 (2018) 108.
- [84] A. Zaraki, M. Ghalambaz, A.J. Chamkha, M. Ghalambaz, D. De Rossi, Theoretical analysis of natural convection boundary layer heat and mass transfer of nanofluids: effects of size, shape and type of nanoparticles, type of base fluid and working temperature, *Adv. Powder Technol.* 26 (2015) 935–946.
- [85] M. Sabour, M. Ghalambaz, A. Chamkha, Natural convection of nanofluids in a cavity: criteria for enhancement of nanofluids, *International Journal of Numerical Methods for Heat & Fluid Flow* 27 (2017) 1504–1534.
- [86] T.C. Paul, A.K.M.M. Morshed, E.B. Fox, J.A. Khan, Experimental investigation of natural convection heat transfer of Al<sub>2</sub>O<sub>3</sub> Nanoparticle Enhanced Ionic Liquids (NEILs), *Int. J. Heat Mass Transf.* 83 (2015) 753–761.
- [87] K.M. Shirvan, S. Mirzakhani, A.J. Chamkha, M. Mamourian, Numerical simulation and sensitivity analysis of effective parameters on natural convection and entropy generation in a wavy surface cavity filled with a nanofluid using RSM, *Numerical Heat Transfer, Part A* 70 (2016) 1157–1177.
- [88] G.A. Sheikhzadeh, A. Aghaei, S. Soleimani, Effect of nanoparticle shape on natural convection heat transfer in a square cavity with partitions using water–SiO<sub>2</sub> nanofluid, *Transport Phenomena in Nano and Micro Scales* 6 (2018) 27–38.
- [89] T.A. Alkanhal, M. Sheikholeslami, M. Usman, R. Haq, A. Shafee, A.S. Al-Ahmadi, I. Tlili, Thermal management of MHD nanofluid within the porous medium enclosed in a wavy shaped cavity with square obstacle in the presence of radiation heat source, *Int. J. Heat Mass Transf.* 139 (2019) 87–94.
- [90] A.S. Dogonchi, M. Waqas, D.D. Ganji, Shape effects of copper-oxide (CuO) nanoparticles to determine the heat transfer filled in a partially heated rhombus enclosure: CVFEM approach, *International Communications in Heat and Mass Transfer* 107 (2019) 14–23.
- [91] A.S. Dogonchi, F. Selimefendigil, D.D. Ganji, Magneto-hydrodynamic natural convection of CuO–water nanofluid in complex shaped enclosure considering various nanoparticle shapes, *International Journal of Numerical Methods for Heat & Fluid Flow* 29 (2019) 1663–1679.
- [92] A. Rahimi, P. Azarikhan, A. Kasaeipoor, E.H. Malekshah, L. Kolsi, Lattice Boltzmann simulation of free convection's hydrothermal aspects in a finned/multi-pipe cavity filled with CuO–water nanofluid, *International Journal of Numerical Methods for Heat & Fluid Flow* 29 (2019) 1058–1078.
- [93] T.K. Nguyen, M. Usman, M. Sheikholeslami, R.U. Haq, A. Shafee, A.K. Jilani, I. Tlili, Numerical analysis of MHD flow and nanoparticle migration within a permeable space containing non-equilibrium model, *Physica A* 537 (2020), 122459.
- [94] A.S. Dogonchi, M. Hashemi-Tilehnoe, M. Waqas, S.M. Seyyedi, I.L. Animasaun, D.D. Ganji, The influence of different shapes of nanoparticle on Cu–H<sub>2</sub>O nanofluids in a partially heated irregular wavy enclosure, *Physica A* 540 (2020) 123034.
- [95] A. Shahsavari, M. Rashidi, M.M. Mosghani, D. Toghraye, P. Talebizadehsardari, A numerical investigation on the influence of nanoadditive shape on the natural convection and entropy generation inside a rectangle-shaped finned concentric annulus filled with boehmite alumina nanofluid using two-phase mixture model, *J. Therm. Anal. Calorim.* 141 (2020) 915–930.
- [96] M. Gholinia, S.A.H.K. Moosavi, S. Gholinia, D.D. Ganji, Numerical simulation of nanoparticle shape and thermal ray on a CuO/C<sub>2</sub>H<sub>6</sub>O<sub>2</sub>–H<sub>2</sub>O hybrid base nanofluid inside a porous enclosure using Darcy's law, *Heat Transfer–Asian Research* (2020) <https://doi.org/10.1002/htj.21541> (In Press).
- [97] M. Gholinia, S.A.H.K. Moosavi, M. Pourfallah, S. Gholinia, D.D. Ganji, A numerical treatment of the TiO<sub>2</sub>/C<sub>2</sub>H<sub>6</sub>O<sub>2</sub>–H<sub>2</sub>O hybrid base nanofluid inside a porous cavity under the impact of shape factor in MHD flow, *International Journal of Ambient Energy* (2020) <https://doi.org/10.1080/01430750.2019.1614996> (In Press).
- [98] D.D. Vo, M. Hedayat, T. Ambreen, S.A. Shehzad, M. Sheikholeslami, A. Shafee, T.K. Nguyen, Effectiveness of various shapes of Al<sub>2</sub>O<sub>3</sub> nanoparticles on the MHD convective heat transportation in porous medium: CVFEM modelling, *J. Therm. Anal. Calorim.* 139 (2020) 1345–1353.
- [99] H. KhakRah, M. Mohammadi, P. Hooshmand, N. Bagheri, E.H. Malekshah, Free convection analysis in a Γ-shaped heat exchanger using lattice Boltzmann method employing second law analysis and heatmap visualization, *International Journal of Numerical Methods for Heat & Fluid Flow* 29 (2019) 3056–3074.
- [100] G. Sowmya, B.J. Gireesha, B.C. Prasannakumara, Scrutinization of different shaped nanoparticle of molybdenum disulfide suspended nanofluid flow over a radial porous fin, *International Journal of Numerical Methods for Heat & Fluid Flow* 30 (2019) 3685–3699.
- [101] S.S. Ghadikolaei, M. Yassari, H. Sadeghi, Kh. Hosseinzadeh, D.D. Ganji, Investigation on thermophysical properties of TiO<sub>2</sub>–Cu/H<sub>2</sub>O hybrid nanofluid transport dependent on shape factor in MHD stagnation point flow, *Powder Technol.* 322 (2017) 428–438.



- [102] S.S. Ghadikolaei, Kh. Hosseinzadeh, D.D. Ganji, Investigation on three dimensional squeezing flow of mixture base fluid (ethylene glycol–water) suspended by hybrid nanoparticle ( $\text{Fe}_3\text{O}_4$ –Ag) dependent on shape factor, *J. Mol. Liq.* 262 (2018) 376–388.
- [103] S. Dinarvand, M.N. Rostami, I. Pop, A novel hybridity model for  $\text{TiO}_2$ –CuO/water hybrid nanofluid flowover a static/moving wedge or corner, *Sci. Rep.* 9 (2019), 16290.
- [104] A. Bhattad, J. Sarkar, Effects of nanoparticle shape and size on the thermohydraulic performance of plate evaporator using hybrid nanofluids, *J. Therm. Anal. Calorim.* (2020) <https://doi.org/10.1007/s10973-019-09146-z> (In Press).
- [105] M. Benkhedda, T. Boufendi, T. Tayebi, A.J. Chamkha, Convective heat transfer performance of hybrid nanofluid in a horizontal pipe considering nanoparticles shapes effect, *J. Therm. Anal. Calorim.* 140 (2020) 411–425.
- [106] A.H. Ghobadi, M.G. Hassankolaei, A numerical approach for MHD  $\text{Al}_2\text{O}_3$ – $\text{TiO}_2$ /H<sub>2</sub>O hybrid nanofluids over a stretching cylinder under the impact of shape factor, *Heat Transfer–Asian Research* (2020) <https://doi.org/10.1002/htj.21591> (In Press).
- [107] A. Aziz, W. Jamshed, Y. Ali, M. Shams, Heat transfer and entropy analysis of Maxwell hybrid nanofluid including effects of inclined magnetic field, Joule heating and thermal radiation, *Discrete and Continuous Dynamical Systems Series S* 13 (2020) 2667–2690.
- [108] S.S. Ghadikolaei, Kh. Hosseinzadeh, D.D. Ganji, Investigation on ethylene glycol–water mixture fluid suspend by hybrid nanoparticles ( $\text{TiO}_2$ –CuO) over rotating cone with considering nanoparticles shape factor, *J. Mol. Liq.* 272 (2018) 226–236.
- [109] S.S. Ghadikolaei, M. Gholinia, 3D mixed convection MHD flow of GO– $\text{MoS}_2$  hybrid nanoparticles in  $\text{H}_2\text{O}$ –( $\text{CH}_2\text{OH}$ )<sub>2</sub> hybrid base fluid under effect of H<sub>2</sub> bond, *International Communications in Heat and Mass Transfer* 110 (2020), 104371.
- [110] E.N. Maraj, Z. Iqbal, E. Azhar, Z. Mehmood, A comprehensive shape factor analysis using transportation of  $\text{MoS}_2$ – $\text{SiO}_2$ /H<sub>2</sub>O inside an isothermal semi vertical inverted cone with porous boundary, *Results in Physics* 8 (2018) 633–641.
- [111] S.S. Ghadikolaei, M. Gholinia, M.E. Hoseini, D.D. Ganji, Natural convection MHD flow due to  $\text{MoS}_2$ –Ag nanoparticles suspended in  $\text{C}_2\text{H}_6\text{O}_2$ –H<sub>2</sub>O hybrid base fluid with thermal radiation, *J. Taiwan Inst. Chem. Eng.* 97 (2019) 12–23.
- [112] M. Sahu, J. Sarkar, Steady–state energetic and exergetic performances of single–phase natural circulation loop with hybrid nanofluids, *J. Heat Transf.* 141 (2019) 082401.